Pacific Northwest
NATIONAL LABORATORY

PNNL-32478 Rev 1.0

Radiological Characterization of Uranium Decay Products in LEU U-10Mo Before and After Heat Treatment

February 2024

D Calderin Morales
ZF Huber
C Arendt
CZ Soderquist

U.S. DEPARTMENT OF ENERGY

Prepared for the U.S. Department of Energy
under Contract DE-AC05-76RL01830

DISCLAIMER

PACIFIC NORTHWEST NATIONAL LABORATORY
operated by
BATTELLE
for the
UNITED STATES DEPARTMENT OF ENERGY
under Contract DE-AC05-76RL01830

Printed in the United States of America

Available to DOE and DOE contractors from
the Office of Scientific and Technical Information,
P.O. Box 62, Oak Ridge, TN 37831-0062
www.osti.gov
ph: (865) 576-8401
fox: (865) 576-5728
email: reports@osti.gov

Available to the public from the National Technical Information Service
5301 Shawnee Rd., Alexandria, VA 22312
ph: (800) 553-NTIS (6847)
or (703) 605-6000
email: info@ntis.gov
Online ordering: http://www.ntis.gov

Document History Summary

Formal revisions to this document or evidence of periodic review are listed below.

Rev. #	Comments	Effective Date
0.0	Initial issue.	1/3/22
1.0	Revised figure 3, removed “Project Controlled Information” markings, clarified conclusion.	tbd

Radiological Characterization of Uranium Decay Products in LEU U-10Mo Before and After Heat Treatment

February 2024

D Calderin Morales
ZF Huber
C Arendt
CZ Soderquist

Prepared for
the U.S. Department of Energy
under Contract DE-AC05-76RL01830

Pacific Northwest National Laboratory
Richland, Washington 99354

Executive Summary

Fuel for the U.S. high-performance research reactor fleet is undergoing significant development as the United States moves away from using highly enriched uranium dispersion fuels. The proposed fuel is a high-density, low-enriched uranium (LEU, 19.75 wt% U-235) alloyed with ten weight percent molybdenum fuel (known as LEU U-10Mo). The LEU U-10Mo fuel samples studied in this report were made by down-blending highly enriched uranium with a master alloy, which is cast from molybdenum rods and depleted uranium, via vacuum induction melting and then casting. The final cast fuel should have 10 wt% molybdenum and a uranium enrichment of 19.75 wt% U-235. From casting to final fuel element formation, the LEU U-10Mo material undergoes several thermomechanical processing steps to attain the desired form and meet the specifications of the fuel plate.

The present work focuses on methods to detect, identify, and quantify the factors behind varying levels of loose contamination on bare LEU U-10Mo after heat treatment (homogenization). Contamination level variation is suspected to originate from ingrowth of uranium decay products over time, together with diffusion and accumulation on the outer surface.

To characterize the uranium decay products ingrown in the alloy without interference from uranium and molybdenum, a source-sample of LEU U-10Mo (two years after processing, analyzed as-is) was dissolved in concentrated acid. The uranium and molybdenum were separated out by anion exchange, leaving the decay chain products in solution. The solution was analyzed by gamma and alpha spectrometry. The gamma spectra shown a cluttered spectrum with minor components of the decay chains and high uncertainty on the nuclide identification. The alpha spectrometry results clearly showed ingrowth of Th-228, Ra-224, Rn-220, Po-216 (daughters of U-232/236), and Th-230 from U-234. The level of ingrown of Th-230 activity is approximately equal to the ingrowth expected from U-234 after two years' decay. Presence of polonium-215 in the alpha spectrum proves that Ac-227 and likely its parent Pa-231 were also present.

It was also hypothesized that thermal processing influenced diffusion of uranium decay products from the interior to the surface of the alloy. To test this hypothesis, a sample was thermally treated in a furnace at 900°C for 144 hours under vacuum, while another sample (from the same material) was kept as control. Next, the samples underwent controlled etching to remove thin layers approximately 5 microns thick. This step was repeated two more times to quantify the progeny levels at three different depths in the sample.

The surface beta/gamma and alpha activities of the homogenized sample were higher than the activities measured for the same sample before heat treatment (homogenization). Of significance, the homogenized sample had 51% less mass; however, it exhibited more surface activity (alpha and beta/gamma). The alpha activity increased by 12% and the beta/gamma activity increased by a factor of 2.5. The beta-to-alpha activity ratio also increased by a factor of 1.50.

The thermal processing experiment showed that the surface of the heat-treated sample had more progeny activity than the surface of the non-heat-treated sample per layer etched. This behavior was noticed for Th-234/Pa-234m, Th-230, Th-228, and Po-215. The activity was higher at the first surface etched from the heat-treated sample, while subsequently etched layers from the same sample seemed to be "depleted" in decay products relative to proportions that would be expected. The mechanism involved can potentially be attributed to vacancy movements

among the atoms. In these vacancy movements, atoms exchange positions or move collectively via grain boundary diffusion, chemical diffusion, and intrinsic diffusion. Future research will investigate which mechanism is dominant.

Acknowledgments

This research was funded by the U.S. Department of Energy and the National Nuclear Security Administration's Office of Material Management and Minimization. The research was performed at Pacific Northwest National Laboratory under contract DE-AC05-76RL01830.

Acronyms and Abbreviations

CAM	continuous air monitoring
COC	Certificate of Conformance
CV	coefficient of variation
DU	depleted uranium
LEU	low-enriched uranium at 19.75 wt% U-235
LEU U-10Mo	alloy of 90 wt% low-enriched uranium and 10 wt% molybdenum
U-10Mo	uranium alloyed with 10 wt% molybdenum
VAF	vacuum annealing furnace

Contents

Executive Summary ii
Acknowledgments iv
Acronyms and Abbreviations v
Contents vi
1.0 Introduction 1
1.1 Uranium Decay Progeny 1
2.0 Objective 3
3.0 Materials and Methods 5
3.1 Method to Characterize the Contamination Levels, Dose Rates, and Progeny in LEU U-10Mo Metal Alloy 5
3.1.1 Method to Calculate the Alpha Activity and Ingrowth in LEU U-10Mo 5
3.1.2 Method to Measure Contamination Levels (Alpha and Beta) 6
3.1.3 Method to Measure Dose Rates (Beta, Gamma) 8
3.1.4 Methods for Characterizing Isotopes in LEU U-10Mo 8
3.2 Methods to Characterize the Contamination Levels, and Progeny Diffusion After Thermal Treatment 10
3.2.1 Surface Etching Approach 10
3.2.2 Continuous Air Monitoring Before and After Heat Treatment 12
4.0 Results and Discussion 14
4.1 Contamination Levels, Dose Rates, and Progeny Characterization in LEU U-10Mo Alloy 14
4.1.1 LEU U-10Mo Activity and Decay Analysis Results 14
4.1.2 Radiological Survey Results on LEU U-10Mo Samples 15
4.1.3 Beta and Gamma Dose Rates 17
4.1.4 Progeny Characterization 18
4.2 Contamination Levels and Progeny Diffusion After Thermal Treatment Results 23
4.2.1 Radiological Survey of Homogenized Sample 23
4.2.2 Progeny Analysis After Homogenization 24
4.2.3 Gamma Spectroscopy Results 26
4.2.4 Alpha Spectroscopy Results 26
4.2.5 Continuous Air Monitoring Results 30
5.0 Conclusions 32
6.0 Quality Assurance 34
7.0 References 35

Figures

Figure 1. Left to Right (with minor branches ignored): Uranium (U-238, 4n+2), Actinium (U-235, 4n+3), and Thorium Decay Series (Th-232 from U-236 and U-232, 4n) (Data from Johnson and Birky [2012]) 2
Figure 2. Hypothesized Behavior 4
Figure 3. Cast Plate Designations. The sample areas used are outlined in red. 6
Figure 4. Cut Sample (left); Main Sample (right) 9
Figure 5. Uranium Decay Products Separation by Anion Exchange in Hydrochloric Acid 9
Figure 6. Vacuum Annealing Furnace. Outside (left); inside (right) hot zone, 16" × 16" × 32". Manufacturer is Thermal Technology LLC. 11
Figure 7. Sketch of Etching Target per Layer 12
Figure 8. Post-Homogenization Sample Etching 12
Figure 9. CAM Configuration 13
Figure 10. Decay Chains of LEU U-10Mo Uranium First Nuclides (Data from Johnson and Birky [2012]) 15
Figure 11. Gamma Spectroscopy Results for Bottom 1 Sample 19
Figure 12. Bottom 1 Sample Thorium Analysis Results 21
Figure 13. Bottom 1 Sample Neptunium Analysis Results 22
Figure 14. Bottom 1 Sample Plutonium Analysis Results 22
Figure 15. Top Sample after Homogenization. Left: longitudinal view; right: cross-sectional view 24
Figure 16. Thorium Alpha Spectrum for Surface Layer Etched from Homogenized Top Sample and As-Cast Bottom Sample 29
Figure 17. Thorium Alpha Spectrum for Subsurface Layer Etched from Homogenized Top Sample and As-Cast Bottom Sample 29
Figure 18. Thorium Alpha Spectrum for Deeper Layer Etched from Homogenized Top Sample and As-Cast Bottom Sample 30
Figure 19. CAM as a Function of Time/Progression of Events 31

Tables

Table 1. LEU U-10Mo Reported Uranium Isotopic Content 5
Table 2. Alpha Activity Analysis in LEU U-10Mo 14
Table 3. LEU U-10Mo Calculated Fractions of Initial Ingrown Longer Progeny Since Casting 15
Table 4. Samples' Dimensions, Volume, Mass, and Density 15
Table 5. Top Sample Radiological Survey Results 16
Table 6. Bottom Sample Radiological Survey Results 17
Table 7. Beta-Gamma Dose Rate for Top and Bottom Samples at Contact 18
Table 8. Cut Sample Mass 18
Table 9. Alpha Spectroscopy LEU U-10Mo Thorium Analysis Results 20
Table 10. Alpha Spectroscopy LEU U-10Mo Transuranic Analysis Results 21
Table 11. Post-Homogenization Bottom Sample Radiological Survey Results 23
Table 12. Dimensional Measurements of Samples before Surface Etching 25
Table 13. Mass and Depth Estimation Measurement as a Function of Etching 25
Table 14. Survey Results to Fraction Mass Etched in Dilution 26
Table 15. Gamma Spectroscopy First-Measurement Results Analysis of Th-234/Pa-234m 27
Table 16. Gamma Spectroscopy Second-Measurement Results Analysis of Th-234/Pa-234m 27
Table 17. Alpha Spectroscopy Results and Analysis 28
Table 18. CAM Event Definitions 30

1.0 Introduction

Fuel for the U.S. high-performance research reactor fleet has been undergoing significant development as the United States moves away from using highly enriched uranium fuels. The proposed fuel is a high-density, low-enriched uranium (LEU) at 19.75 wt% U-235 alloyed with 10% weight molybdenum (known as LEU U-10Mo). As part of the fuel development effort, this task studied methods to characterize and understand the LEU U-10Mo radiological dose rate variability as a function of homogenization heat treatment. This problem is considerably more prevalent on uranium surfaces before the hot roll bonding of a zirconium interlayer onto the metal. Identifying why thermal processing affects the radiation dose rate and contamination levels of LEU U-10Mo is critical to the fuel-fabrication pillar and the Reactor Conversion Program because handling larger quantities of materials is expected. Unanticipated radiological incidents of this nature have caused schedule delays and would result in increased cost. During the plate demonstration process, the program explored two-step, bare hot rolling to improve the metallurgical properties of the LEU U-10Mo. However, elevated loose alpha and beta contamination were detected during de-canning (after hot rolling), causing the work to stop. Results from studying this radiological and material science phenomenon will advance both our understanding of the isotopic composition of the LEU U-10Mo fuel and the formation and diffusion of uranium decay products toward the surfaces of these fuel plates.

The LEU U-10Mo alloy studied in this report was made by down-blending highly enriched uranium, depleted uranium (DU), and master alloy[1] in proportions to produce an alloy of 90 wt% uranium and 10 wt% molybdenum, in which the uranium is enriched to 19.75 wt% U-235 (INL 2013). The bare cast plates are cut into ingots. Then, the ingots are sized to billets and the billets are rolled to foils. A zirconium layer and cladding are added to form the plates that go into the desired assembly configuration. During these steps, several heat treatments are conducted to adjust the metallurgical characteristics of the alloy. Between these thermal processes, spikes in alpha and beta counts are detected, at the surface of the bare alloy and by smear samples.

1.1 Uranium Decay Progeny in LEU U-10Mo

The LEU U-10Mo alloy analyzed in this report has U-238, U-236, U-235, U-234 and traces of U-232 in its isotopic composition (Section 3.1.1). The rate of ingrowth of the uranium decay products is dominated by the mass composition of long-lived members in the starting uranium; these are marked with bolder lines in Figure 1 (Johnson and Birky 2012). This figure shows the decay product chain for uranium series (U-238, 4n+2), actinium series (U-235, 4n+3), and thorium series (Th-232 from U-236 and U-232, 4n).

The rate of uranium decay product ingrowth will depend on the time since the LEU U-10Mo was last processed—in this case, cast. Over time, uranium's short-lived members will reach equilibrium with the previous long-lived members. For example, after six months, Th-234/Pa-234m will reach activity equilibrium with U-238 (AMC 1989). The uranium decay products include a combination of alpha, beta, and gamma emitters, which show the need to perform both alpha and gamma spectroscopy to identify and quantify the elements in the decay chain.

[1] The master alloy is produced using vacuum induction melting and casting to produce a DU + Mo rod in the form of a log.

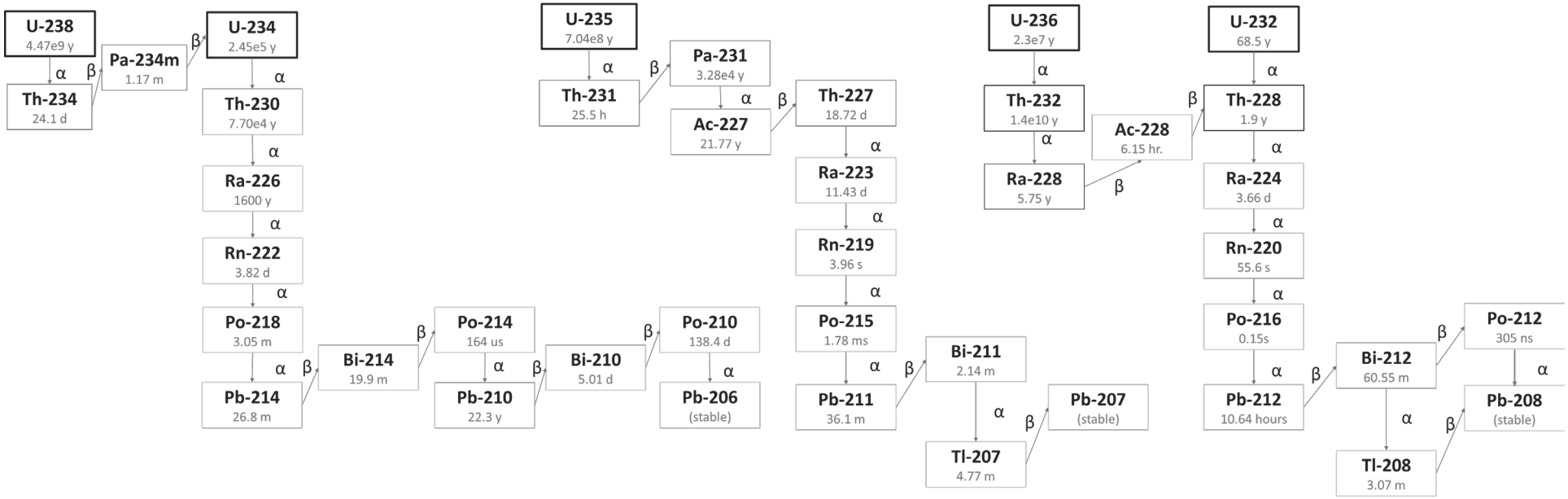

Figure 1. Left to Right (with minor branches ignored): Uranium (U-238, 4n+2), Actinium (U-235, 4n+3), and Thorium Decay Series (Th-232 from U-236 and U-232, 4n) (Data from Johnson and Birky [2012])

2.0 Objective

This research focused on understanding how homogenization and etch-cleaning processes influence the external radiation dose rate and contamination levels on bare LEU U-10Mo metal forms (ingots, billets, and foils). It aims to make sure that thermal processing of bare ingots, billets, and foils through plate finishing does not adversely affect the underlying assumptions related to the external radiation dose rate and contamination levels (measured by removable and fixed contamination).

The focus of this research is on the homogenization step of the LEU U-10Mo fabrication process.

The hypotheses that are the bases of this research are briefly described below:

- *Hypothesis 1*. The increase in alpha and beta counts in LEU U-10Mo metal observed immediately after homogenization is a direct result of uranium progeny diffusing to the surface as a function of temperature and time.
- *Hypothesis 2.* The decrease in alpha and beta counts in LEU U-10Mo metal observed a longer time after homogenization results from a combination of uranium progeny decay and shielding by an oxide/carbide layer that forms during cooling.
- *Hypothesis 3.* The sources of airborne particulates are uranium oxides and uranium progeny.
- *Hypothesis 4.* The progeny found in the alloy will increase as a function of time elapsed since the last processing step.

These processes are illustrated in Figure 2.

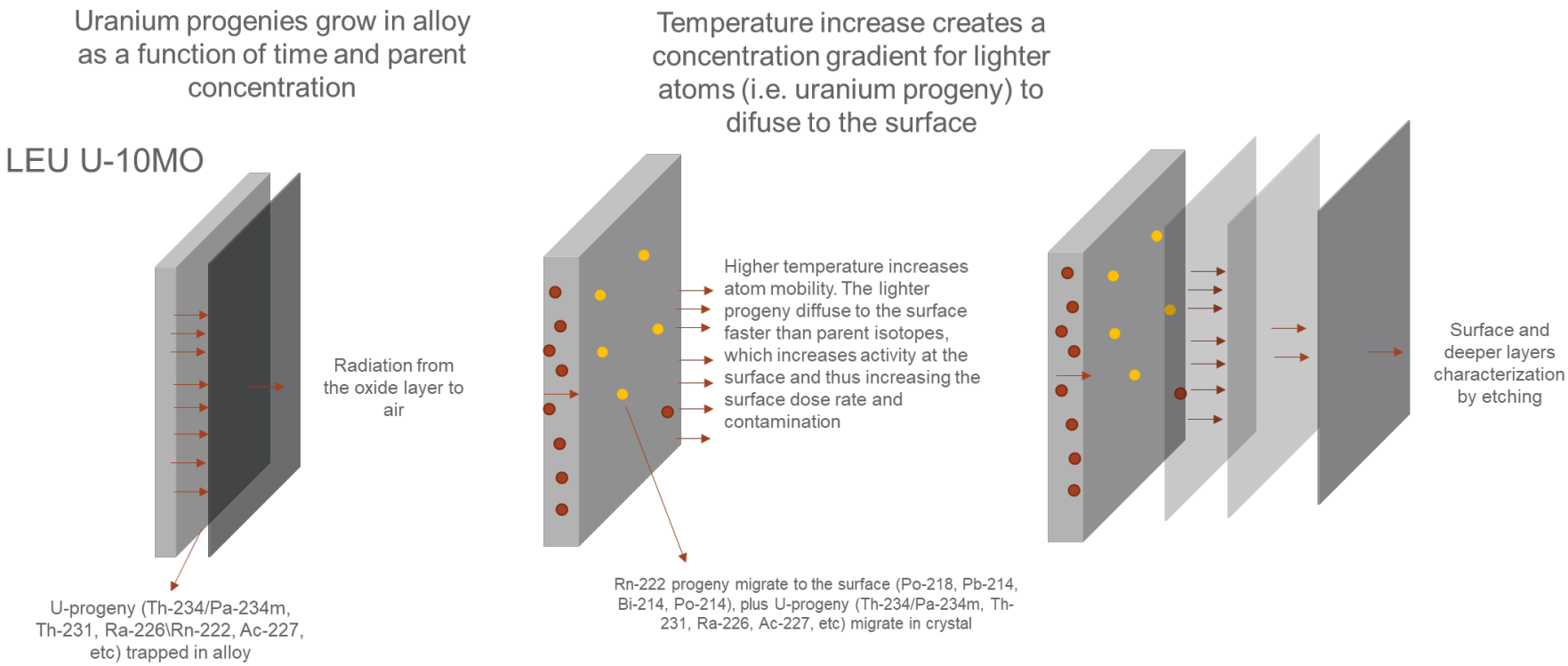

Figure 2. Hypothesized Behavior

3.0 Materials and Methods

The initial focus of the research was to perform radiological characterization and study the diffusion of uranium decay products in LEU U-10Mo before and after homogenization. This thermal process is performed in a vacuum annealing furnace (VAF) with a high-purity argon-backfill quick-quenching capability. The processing parameters consist of pressurizing the vacuum chamber at approximately 1 mTorr while increasing the temperature to 900°C, and then maintaining these parameters for 144 hours. No gas purge during preheating is performed. Upon completion, the pressure in the chamber is increased from 1 mTorr to 760 Torr. As the temperature in the chamber decreases, argon is metered in to maintain the pressure within the 745–760 Torr range.

3.1 Method to Characterize the Contamination Levels, Dose Rates, and Progeny in LEU U-10Mo Metal Alloy

3.1.1 Method to Calculate the Alpha Activity and Ingrowth in LEU U-10Mo

The LEU-10Mo alloy used for this research comes from a casting short pour that used the method given in Process Development Standard 1 (COC WR 866218), in which a highly enriched uranium log, master alloy, and DU are melted in a vacuum induction furnace and then cast to form a plate with U-235 enrichment at 19.75wt% of the U). This method is described in Certificate of Conformance (COC) Work Request (WR) 866218. The material is shown in Figure 3. Two cast samples were taken from the same plate, one from the top and the other from the bottom of the plate, each weighing approximately 60 g.

The alloy was cast and analyzed in September 2018 (COC WR 866218). The samples were re-analyzed in February 2021 for uranium decay progeny (i.e., approximately 2.42 years later). The as cast average uranium isotopic mass distribution is shown in Table 1. The U-232 measurement was taken only once and is reported as 3,860 dpm/g-U (COC WR 866218).

Table 1. LEU U-10Mo Reported Uranium Isotopic Content (COC WR 866218)

U Isotope	Average Content (wt%)	Standard Deviation (wt%)
U-238	79.9227	0.0046
U-236	0.0747	0.0006
U-235	19.7897	0.0040
U-234	0.2117	0.0006

The values reported in Table 1 came from the center strip of the plate (Figure 3, golden holes), from which three samples were analyzed. Two vertical strips (left and right) were produced from the plate.

In addition, the left strip was cut into top and bottom samples (highlighted in red in Figure 3), which are the ones used in this study.

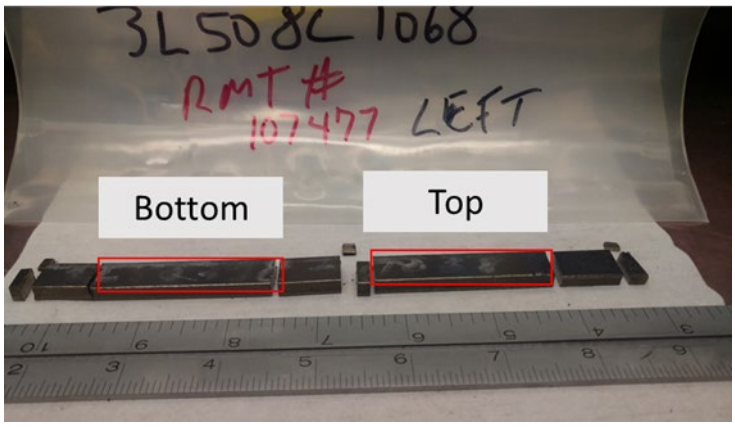

Figure 3. Cast Plate Designations. The sample areas used are outlined in red.

These samples came from Plate 1 of the PD-6 run, which had a short pour and did not generate a hot top (COC WR 866218).

The specific alpha activity of each uranium nuclide was calculated as

$$SA_N = \frac{\lambda_N \times N_A}{MW_N}$$

where λ is the half-life, N_A is Avogadro's number, and *MW* is the molecular weight.

The activity of each nuclide is

$$A_N = SA_N \times wt_N \times wt_{uranium}$$

where wt_N is the weight percent of the nuclide in the uranium and $wt_{uranium}$ is the weight percent of uranium in the alloy. Note that the total uranium composition in the alloy is approximately 90 wt% and the other 10 wt% is molybdenum.

Finally, the activity of the progeny ingrowth is calculated as

$$A_i = A_N(1 - e^{\lambda_i \times t})$$

where A_i is the ingrowth activity from parent A_N, λ_i is the half-life of the progeny *i*, and *t* is the time since casting (or last processing step).

The ingrowth activity analysis will focus on the first long-lived progeny from each uranium isotope identified in Table 1, plus U-232.

Method to Measure Contamination Levels (Alpha and Beta)Alpha and beta particles were detected using a Ludlum Model 43-93 scintillation counter, which can distinguish alpha from beta counts. The beta-gamma efficiency (29.4%) was taken based on a Sr-90/Y-90 calibration source, and the alpha efficiency (14.6%) was taken from Pu-239 calibration source.

Before taking the gross counts, background and gross count characterizations were performed to keep the counting error below 10%. Counting measurements were taken at two points: (1) in contact with the surface and (2) at 1 ft from the surface.

The method described below to measure, calculate, and report radiation count mean and error was reported by Tsoulfanidis (1995).

The process is as follows: let *B* be the number of background counts and *G* the gross sample counts; t_b and t_g are the count times (in minutes) for the background and the sample, respectively. Then, the gross count rate is defined as

$$g = \frac{G}{t_g}$$

The standard error of *g* is

$$\sigma_g = \sqrt{\frac{g}{t_g}}$$

The background rate is then

$$b = \frac{B}{t_b}$$

The standard error of *b* is

$$\sigma_b = \sqrt{\frac{b}{t_b}}$$

Then the net count rate is calculated as

$$r = \frac{G}{t_g} - \frac{B}{t_b}$$

The standard error of the net counts is then

$$\sigma_n = \sqrt{\sigma_g^2 + \sigma_b^2}$$

The counting rate standard error as a percentage is

$$\frac{\sigma_n}{r} \leq 10\%$$

At a 95% confidence (one tail), the net counts can be verified as different from the background.

$$95\%\ C.I. \longrightarrow r \geq 1.65\sigma_n$$

Finally, the net activity will be expressed in disintegrations per minute by

$$r_d = \frac{r}{\eta}$$

where η is the detector's net efficiency.

The net count rates were taken in contact with the surface.

A *t*-test on the net count rate was conducted between the top and bottom samples as shown here (Martin 2012):

$$t_{calc} = \frac{|r_{Top} - r_{Bottom}|}{\sqrt{\sigma^2_{Top} + \sigma^2_{Bottom}}}$$

Note that the sample size is considered large when we are counting radioactive decay events and is a selected length of time over which the number of counts is taken (Cember 2008).

3.1.2 Method to Measure Dose Rates (Beta, Gamma)

The beta/gamma dose rates at the sample surface were measured with a Thermo Scientific RO-20 ionization chamber survey meter. For this equipment, a DU response test yielded a reading correction factor of 3.03 (true/observed). The correction factor for environmental conditions (temperature and pressure) was not required because the calibration was performed on-site, so any fluctuation is minimal and not considered.

This measurement will quantify the beta and gamma dose rates. To do this, first, a measurement is taken with an open window (7 mg/cm^2 shield thickness); then, a second measurement is taken with a closed window (1,000 mg/cm^2 shield thickness), which will attenuate all beta rays, so only gamma rays reach the detector's volume. The beta dose rate in a mixed beta/gamma field is calculated by subtracting the open window (beta + gamma) reading from the closed window (gamma only) reading. The same geometry and distance to the surface are maintained for the two measurements.

3.1.3 Methods for Characterizing Isotopes in LEU U-10Mo

The bottom and top LEU U-10Mo samples were cut into representative pieces (approximately 0.4 g each, Figure 4) and then chemically dissolved. The uranium and molybdenum were separated from the progeny for isotopic analysis via gamma and alpha spectroscopy. These processes are explained below.

Using a wet abrasive saw, samples of LEU-10Mo were cut from the larger top and bottom samples (Figure 4). The saw leaves a shiny metallic surface free of visible residue. Samples for bulk analysis were each weighing about 0.4 g. This process generated five samples: three pieces from the bottom sample and two pieces from the top sample.

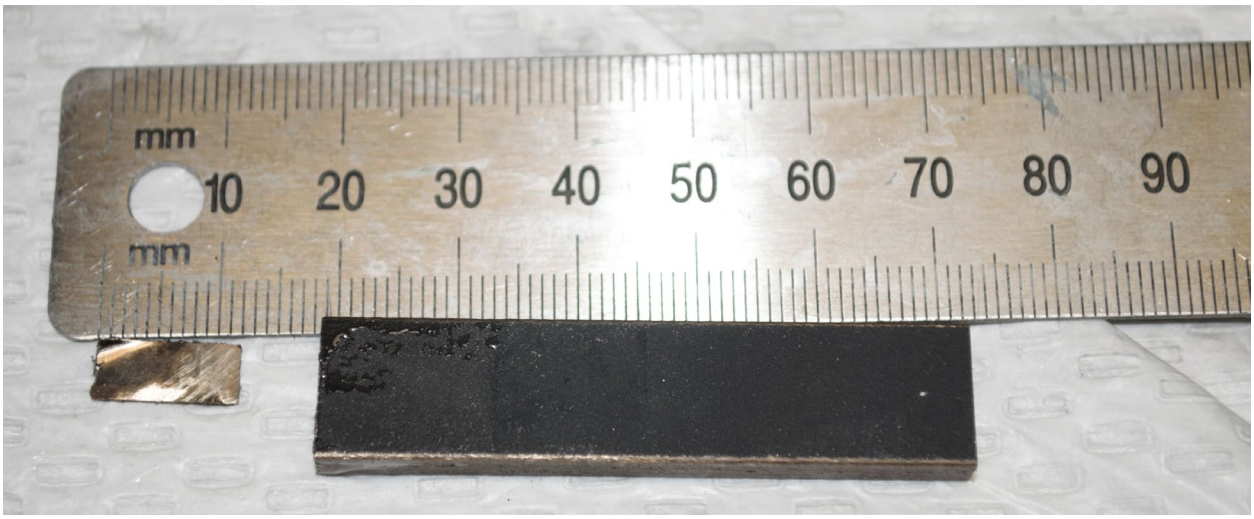

Figure 4. Cut Sample (left); Main Sample (right)

The samples for bulk analysis were weighed, then completely dissolved in concentrated hydrochloric acid with a small amount of hydrogen peroxide added to increase the dissolution rate and maintain a consistent oxidation state of the uranium.

A heavy preponderance of uranium and molybdenum interferes with measurement of the decay chains. Before the decay chains were measured, uranium and molybdenum were removed from the sample solutions by anion exchange in hydrochloric acid (Figure 5). Each sample was passed through a column of anion exchange resin (Bio-Rad MP-1, 50–100 mesh, chloride form). Uranium and molybdenum load strongly onto the resin. Thorium, actinium, radium, and much of the decay chain isotopes pass through and collect, free of uranium and molybdenum, in the beaker below the column. This treatment also removed neptunium and plutonium from the sample solutions. Transuranic elements were eluted from the resin and mounted for alpha spectroscopy as well.

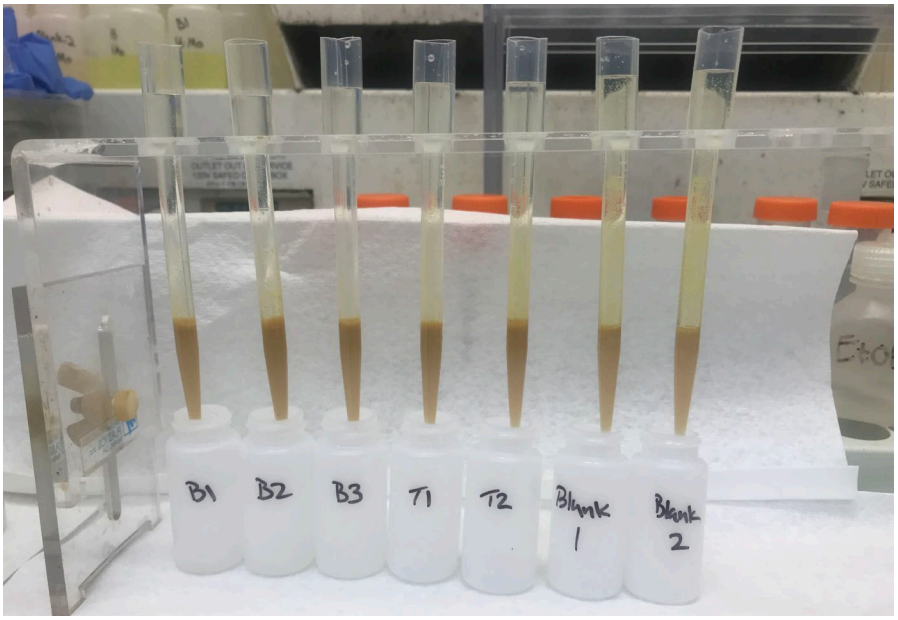

Figure 5. Uranium Decay Products Separation by Anion Exchange in Hydrochloric Acid

3.1.3.1 Method Used for Isotopic Characterization via Gamma Spectroscopy

After uranium was chemically removed from the sample solutions, the solutions were counted for gamma emissions twice, about a week apart, using a gamma spectrometer with a high-purity germanium detector. The samples were counted, and the spectra were evaluated using Genie 2000 software from Mirion Technologies.

3.1.3.2 Method Used for Isotopic Characterization via Alpha Spectroscopy

After gamma counting, each sample was mounted for alpha spectrometry by co-precipitation on 70 µg of NdF_3 on a 2 cm membrane filter. This widely used method (L'Annunziata et al. 2012) measures all alpha-emitting actinide elements. Several prominent members of the decay chains that are hard to measure by gamma spectrometry are easily measured by alpha spectrometry, and the sensitivity of the method is excellent.

To mount a sample for alpha spectrometry, the sample solution was measured into a plastic centrifuge tube. A neodymium carrier was added (50 µg), $TiCl_3$ solution was added to reduce several actinide elements to lower oxidation states, and then hydrofluoric acid was added. A precipitate of NdF_3 formed and carried all actinide elements in the solution as insoluble fluorides. The suspension of NdF_3 was passed through a 2 cm membrane filter, and then washed with water. The NdF_3 collected as a thin, uniform layer on the filter, forming a good source for alpha spectrometry. The filter was washed with water, then attached to a steel counting disk. The filter was allowed to dry, then counted on an alpha spectrometer. The alpha spectrometer has 32 Ortec detectors, running Canberra software, with approximately 20% efficiency per detector.

3.2 Methods to Characterize the Contamination Levels, and Progeny Diffusion After Thermal Treatment

3.2.1 Surface Etching Approach

Surface etching is used to measure and quantify uranium decay progeny that diffuse to the surface of the LEU-10Mo alloy as a result of homogenization (i.e., thermal processing).

Initially, using the cutting procedure described in Section 3.1.4, a sample weighing approximately 20 g was obtained from the top sample. Then, the sample was placed in the VAF and homogenized at a vacuum of 1 mTorr at 900°C for 144 hours (Figure 6). No gas purge during preheating was performed. Upon completion, the pressure in the chamber was increased from 1 mTorr to 760 Torr. As the temperature in the chamber decreases, high-purity argon was used to maintain pressure within a 745–760 Torr range.

The bottom piece was kept as a control (i.e., no heat treatment was applied), and a sample weighing approximately 26 g was cut from it.

The dimensions of each piece were measured for use in surface area calculations, and the pieces were weighed.

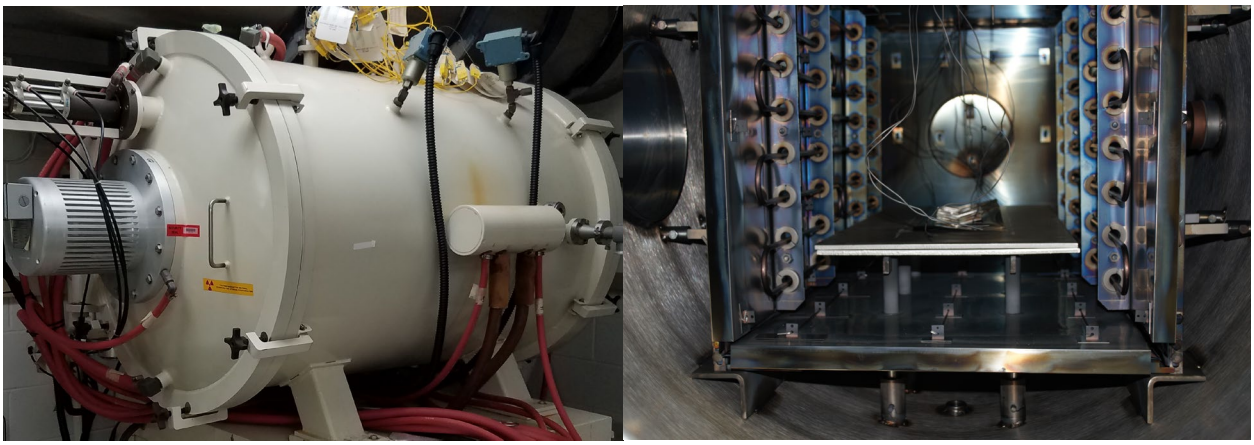

Figure 6. Vacuum Annealing Furnace. Outside (left); inside (right) hot zone, 16" × 16" × 32". Manufacturer is Thermal Technology LLC.

The samples were etched by immersing them in a dilute (six molar) hydrochloric acid/hydrogen peroxide solution to dissolve the surface layer until the remnant mass had decreased by the equivalent of an approximately 5 micron thick layer, and then were removed from solution. After etching, the piece of LEU-10Mo was dried, weighed, and its dimensions recorded (length and width); then, the thickness of the material dissolved was calculated. The same piece of LEU-10Mo was then immersed a second and third time in clean solutions to etch subsequent, deeper layers. During each immersion, more material was removed from the surface, essentially leaving three sample remnants from increasing depths (Figure 7 and Figure 8).

If we assume that the density variation through each etched layer is the same and that the thickness etched was the same across the surfaces, then the following relationship between mass, volume, and thickness removed per etching step can be established:

$$(L - 2 \times \delta) \times (W - 2 \times \delta) \times (H - 2 \times \delta) = \frac{m_L}{m_s} \times V_s$$

where m_s and V_s are the mass and volume of the sample, respectively; m_L is the mass left after etching; and L, W, and H are the length, width, and depth of the sample, respectively. Finally, δ is the depth of the etching on all the surfaces of the sample. This equation was solved iteratively until δ was found.

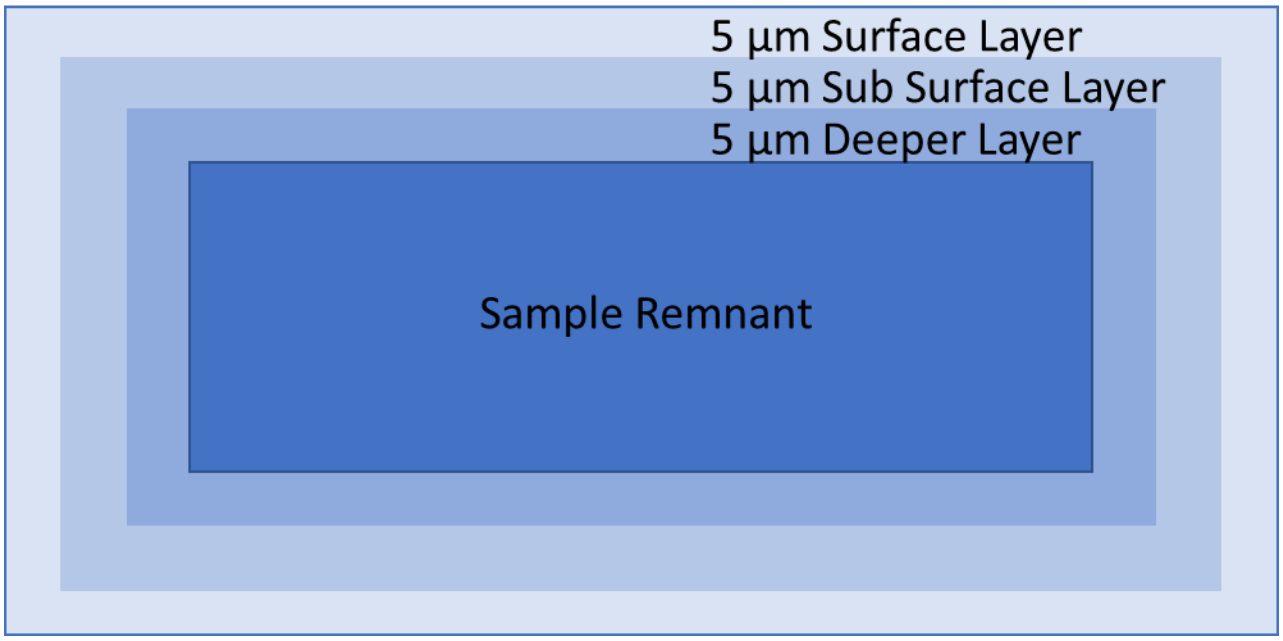

Figure 7. Sketch of Etching Target per Layer

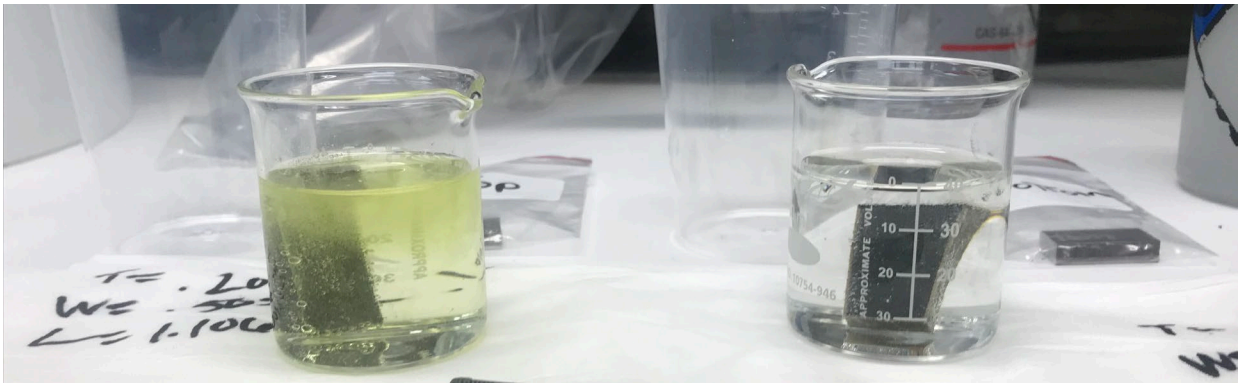

Figure 8. Post-Homogenization Sample Etching. The homogenized sample is shown on the left, while the non-homogenized sample is on the right. Both samples are immersed in a dilute (six molar) hydrochloric acid/hydrogen peroxide solution.

3.2.2 Continuous Air Monitoring Before and After Heat Treatment

This experiment was set up inside a Cole-Parmer glovebox, model 34788-00, where samples were continuously monitored in a closed, controlled environment with a Bladewerx BPM2 beta continuous air monitoring (CAM) detection system and a particulate air monitor. The data collected was analyzed using the software provided by the manufacturer. The configuration is shown in Figure 9.

The measurements were taken by first recording the background radiation level over a long period (4-7 days), after which the bottom sample (i.e., non-homogenized sample) was inserted in the glovebox. Upon completion, this sample was homogenized, radiologically surveyed, and reinserted into the glovebox configuration. In addition, a smear was taken and sent for gamma spectroscopy analysis only.

The CAM-recorded counts were integrated across all channels for the same periods and then divided by the time taken to collect the measurement. The counting were set every 15 minutes each.

The purpose of this step was to evaluate the airborne contamination levels, especially radon, in an undisturbed environment (i.e., similar to inventory) as a function of time.

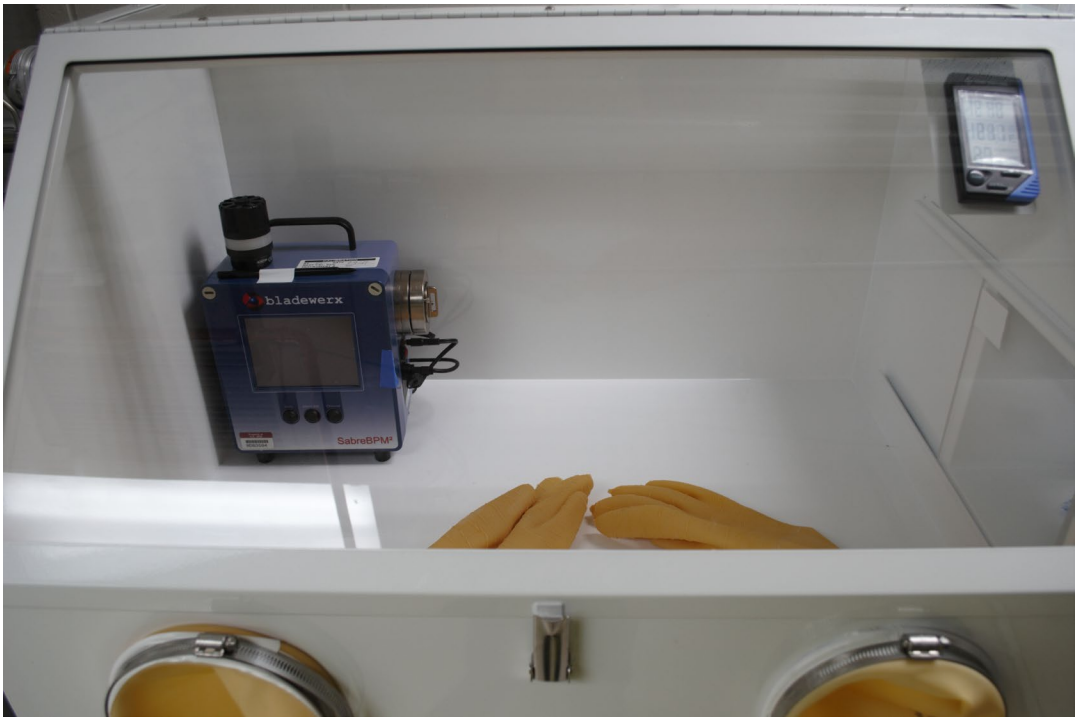

Figure 9. CAM Configuration

4.0 Results and Discussion

4.1 Contamination Levels, Dose Rates, and Progeny Characterization in LEU U-10Mo Alloy

4.1.1 LEU U-10Mo Activity and Decay Analysis Results

Table 2 presents the specific activity based on the uranium nuclide isotopes presented in Table 1. Alpha activity in the LEU U-10Mo is dominated by that of U-234. The total alpha and beta activity values are consistent with those previously reported for 20 wt% enrichments (Hinnefeld et al. 1988, Table 5-4).

Table 2. Alpha Activity Analysis in LEU U-10Mo

U-Isotope	Wt%	Half-life (years)	Specific Alpha Activity (dpm/g-U)	Alpha Activity (dpm/g-alloy)	(%)	Beta Activity[a] (dpm/g-alloy)
U-238	79.9	4.47×10^{9}	7.46×10^{5}	5.35×10^{5}	1.9%	1.07×10^{6}
U-236	0.07	2.34×10^{7}	1.44×10^{8}	9.62×10^{4}	0.3%	0
U-235	19.8	7.04×10^{8}	4.80×10^{6}	8.52×10^{5}	3.1%	8.52×10^{5}
U-234	0.21	2.46×10^{5}	1.38×10^{10}	2.62×10^{7}	94.6%	0
U-232	8.66×10^{-11}	6.89×10^{1}	4.96×10^{13}	3.46×10^{3}[b]	0.0%	0
			Total	2.77×10^{7}	100%	1.92×10^{6}

[a] Assumes equilibrium of U-238 with Th-234/Pa234m (per alpha particle; two beta particles are emitted) and U-235 with Th-231 (per alpha particle; one beta particle is emitted).
[b] The reported value was 3,860 dpm/g-U that then was multiplied by 0.90 g-U/g-alloy.

Figure 10 presents the first nuclides for which ingrowth is prevalent in LEU U-10Mo. Based on decay data, Th-234/Pa234m will reach equilibrium with U-238 in approximately 6 months and Th-231 with U-235 in approximately 6 days (Hinnefeld et al. 1988, Figures 5-4 and 5-5). Because the alloy was cast about two years before this work, they are assumed to be in equilibrium.

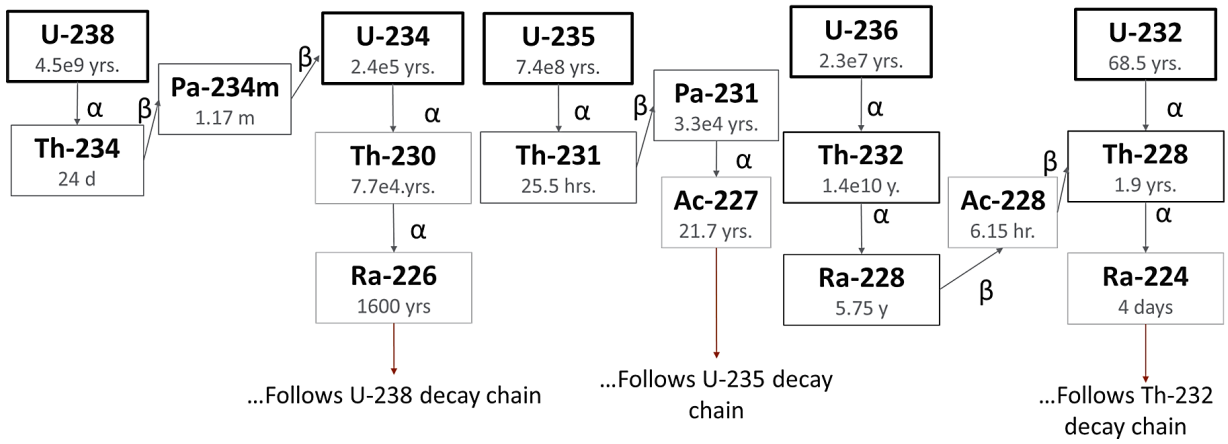

Figure 10. Decay Chains of LEU U-10Mo Uranium First Nuclides (Data from Johnson and Birky [2012])

The calculated ingrowths for the longer half-life nuclides are shown in Table 3. The most significant contributions come from U-234 and U-232 for ingrown Th-230 and Th-228, respectively. These activity values were calculated from the last time the sample was processed (2.4 years before this work).

Table 3. LEU U-10Mo Calculated Fractions of Initial Ingrown Longer Progeny Since Casting

Parent	First Long-Lived Progeny	Half-Life (years)	Specific Activity (dpm/g-alloy)	Fraction Ingrown (2.42 years)	Activity Ingrown (dpm/g-alloy)
U-236	Th-232	1.40×10^{10}	2.44×10^{5}	1.20×10^{-10}	1×10^{-5}
U-235	Pa-231	32,800	1.05×10^{11}	5.11×10^{-5}	44
U-234	Th-230	75,600	4.56×10^{10}	2.22×10^{-5}	581
U-232	Th-228	1.91	1.82×10^{15}	5.84×10^{-1}	2,025

4.1.2 Radiological Survey Results on LEU U-10Mo Samples

Before they were radiologically surveyed, the top and bottom samples were dimensionally inspected and weighed. Then their volume and density were calculated, yielding approximately 16 g/cm^3. These results are presented in Table 4.

Table 4. Samples' Dimensions, Volume, Mass, and Density

Sample ID	Length (cm)	Width (cm)	Thickness (cm)	Volume (cm^3)	Weight (g)	Density (g/cm^3)
Top	5.56	1.22	0.53	3.57	57.56	16.11
Bottom	5.43	1.22	0.53	3.53	55.99	15.85

Results of the radiological surveys performed on the top and bottom samples (before homogenization) are presented in Table 5 and Table 6, respectively. These surveys were performed in contact with the surface of each sample. Their respective beta-gamma and alpha

net count rates were compared using a *t*-test. The *t*-calculated count rates were 25.2 and 43, respectively. These values are greater than the 1.96 confidence criterion, which means there is more than a 95% confidence the differences observed are true. Hence, we can conclude that the top sample has a significantly higher surface net count rate than the bottom sample (for beta and alpha count rates). Note also that the beta-to-alpha activity ratios at the surface are 0.63 for the top sample and 0.69 for the bottom sample. This ratio was expected to be much lower because uranium at 19.75 wt% U-235 is a prevalent alpha emitter, and the beta contribution is mainly from the first decay products. However, because these measurements were taken in contact with the surface, the uranium self-attenuation of beta/gamma particles is lower than alpha particles from inner uranium surface levels.

Table 5. Top Sample Radiological Survey Results

	Units	β-γ Background	α Background
Counts	counts	2,456	12
Time	minutes	5	5
Count Rate	cpm	491.2	2.4
Standard Deviation	cpm	9.9	0.7
		β-γ Gross Counts at Contact	α Gross Counts at Contact
Counts	counts	155,806	122,710
Time	minutes	1	1
Count Rate	cpm	155,806	122,710
Standard Deviation	cpm	394.7	350.3
		β-γ Net Count Rate at Contact	α Net Count Rate at Contact
Count Rate	cpm	155,314.8	122,707.6
Standard Deviation	cpm	394.9	350.3
Coefficient of Variation (CV)	%	0.25%	0.29%
$r > 1.65 \times$ Sigma	cpm	651.5 (Yes)	578.0 (Yes)
		β-γ Activity at Contact	α Activity at Contact
Net Count Rate	cpm	155,314.8	122,707.6
Efficiency[a]	cpm/dpm	0.294	0.146
Efficiency-Standard Deviation[b]	cpm/dpm	0.0001	0.0001
	dpm	528,282	840,463
Activity	Bq	8,805	14,008
	dpm	1,343	2,400
Standard Deviation	Bq	22	40
Beta-to-Alpha Activity Ratio		0.63:1	

[a] The efficiency is based on calibration reports. The beta-gamma efficiency taken was based on a Sr-90/Y-90 calibration source, and the alpha efficiency was taken from Pu-239.
[b] This value was assumed to be small.

Table 6. Bottom Sample Radiological Survey Results

	Units	β-γ Gross Counts at Contact	α Gross Counts at Contact
Counts	counts	142,061	102,512
Time	minutes	1	1
Count Rate	cpm	142,061	102,512
Standard Deviation	cpm	376.9	320.17
		β-γ Net Count Rate at Contact	α Net Count Rate at Contact
Count Rate	cpm	141,570	102,510
Standard Deviation	cpm	377.0	320.18
CV	%	0.27%	0.31%
$r > 1.65 \times$ Sigma	cpm	622.1 (Yes)	528.3 (Yes)
		β-γ Activity at Contact	α Activity at Contact
Net Count Rate	cpm	141,570	102,509
Efficiency[a]	cpm/dpm	0.294	0.146
Efficiency- Standard Deviation[b]	cpm/dpm	0.0001	0.0001
Activity	dpm	481,530	702,121
	Bq	8025	11,702
Standard Deviation	dpm	1283	2193
	Bq	21.4	36.56
Beta-to-Alpha Activity Ratio		0.69:1	

[a] The efficiency is based on calibration reports. The beta-gamma efficiency taken was based on a Sr-90/Y-90 calibration source, and the alpha efficiency was taken from Pu-239.
[b] This value was assumed to be small.

4.1.3 Beta and Gamma Dose Rates

The samples' beta dose rates are presented in Table 7. As expected, the beta dose rate is lower than that of DU (~200 mrad/h; DOE 2000) because the enrichment (~19.75 wt% U-235) leaves less U-238 by mass than that in DU, so the beta dose-rate contribution from Th-234/Pa-234m is also less. Additionally, LEU U-10Mo is 90 wt% uranium and 10 wt% molybdenum. Molybdenum also has a relatively high density (~10.3 g/cm^3) that will contribute to a self-absorption of beta particles at the fuel surface, which results in lower beta dose rates than those from a 100% uranium fuel.

Table 7. Beta-Gamma Dose Rate for Top and Bottom Samples at Contact

Description	Value	Units
Open window at contact gross dose rate	22	mR/h
Closed window net dose rate	0.05[a]	mR/h
Beta dose rate	22	mR/h
Correction Factor	3.03	true/observed
Beta corrected	66.66	mrad/h

[a] Reading matched background levels.

The gamma dose rate (measured with a closed window) was at background levels, which indicates that not enough material is present to generate a significant gamma dose rate. To obtain a meaningful gamma dose rate, this measurement should be performed in facilities that handle bulk quantities of LEU U-10Mo material.

4.1.4 Progeny Characterization

Table 8 presents the final weights of the samples cut before dissolution. These samples were used for characterization via gamma and alpha spectroscopy.

Table 8. Cut Sample Mass

Sample ID	Sample Mass (g)
Bottom 1	0.3192
Bottom 2	0.4668
Bottom 3	0.4454
Top 1	0.3918
Top 2	0.4347

4.1.4.1 Gamma Spectroscopy Results

Figure 11 presents the gamma spectrum of the Bottom 1 sample, which shows many of the major components of the decay chains; however, those same decay chains occur naturally and always appear in the detector background. Background subtraction makes the gamma count less sensitive and increases uncertainty in the measurements. The minor components of the decay chains are hard to measure accurately by gamma measurement instruments. The spectra for the other samples are similar to the one presented, hence not shown in this report.

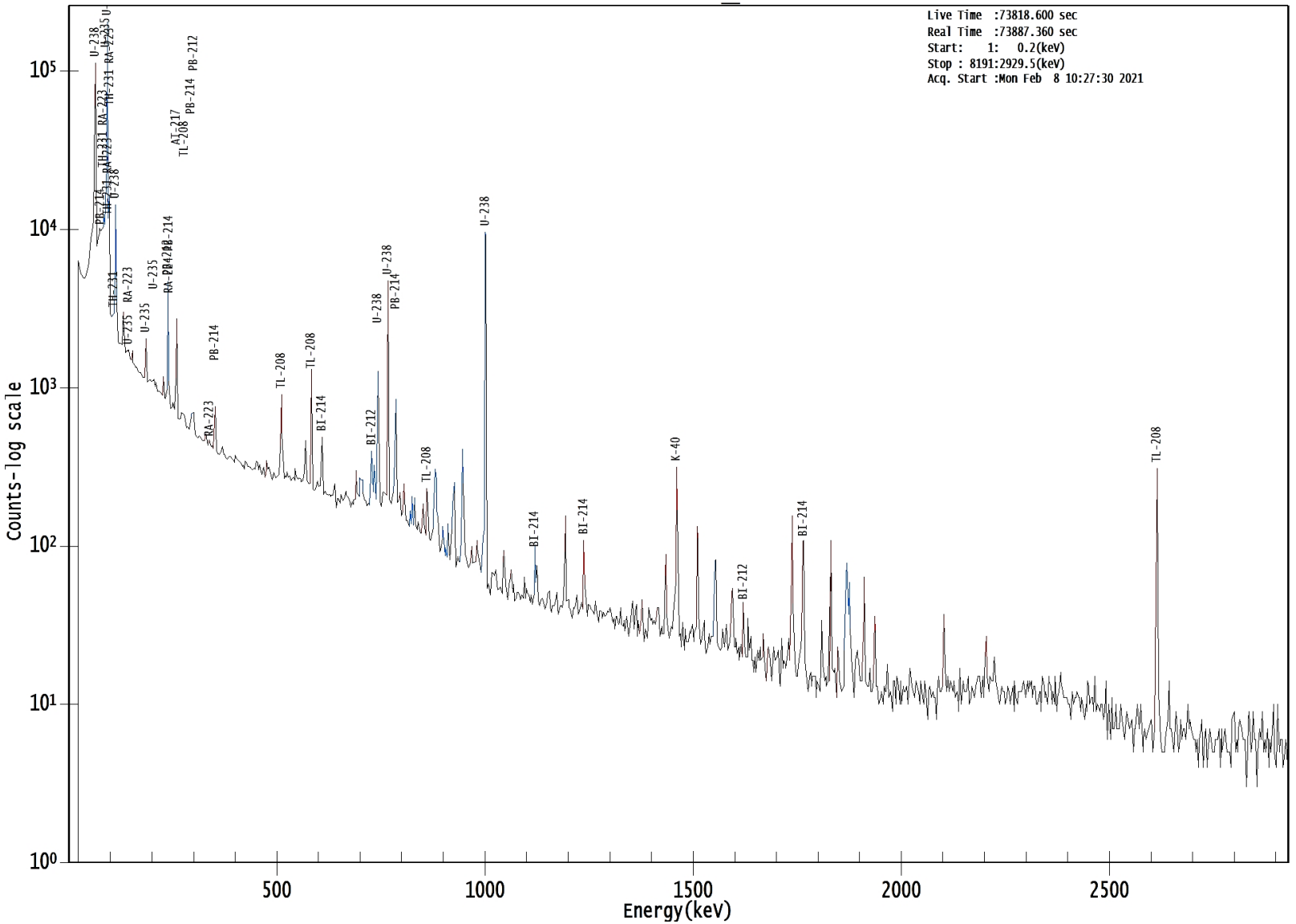

Figure 11. Gamma Spectroscopy Results for Bottom 1 Sample

4.1.4.2 Alpha Spectroscopy Results

Table 9 and Table 10 present the results of the alpha spectroscopy analysis for thorium and transuranic elements in dpm per gram of LEU U-10Mo. Th-232 activity was expected to be low because of the long half-life of the U-236 parent. For Th-230 and Th-228, the results show low variability in bulk activity among the top and bottom samples analyzed. At the bulk sample level, there were no noticeable alpha activity differences among the thorium decay progeny present in the samples analyzed.

The measured Th-230 activity approximates (-8% smaller) to the activity predicted by ingrowth in Table 3. This result indicates that the Th-230 ingrown since the alloy was cast and that the uranium decay progeny contribution from older feedstock used for casting fabrication is minimal in the as cast plates. However, this result does not consider recycling of returns and retains in the decay product final distribution.

In the case of Th-228, the activity measured is less than the one predicted in Table 3. This discrepancy can be attributed to some activity or material lost in the chemistry preparation or uncertainties in casting dates, sample size or uniform distribution in the alloy. In the future, this discrepancy will be investigated by performing mass spectrometry analysis on samples before analyzing them for progeny ingrowth.

Table 10 presents the transuranic composition of the samples. These results indicate the feedstock for the alloy came from recycled uranium (Hinnefeld et al. 1988). The Np-237 activity is relatively constant with low variability across samples. Note that for Pu-239+240 there was a low (Bottom 2 sample) and a peak activity value (Top 2 sample). Fluctuations in the Pu-239 activity may indicate that the distribution of plutonium is not homogeneous in the samples. This process will be studied further in future research.

Table 9. Alpha Spectroscopy LEU U-10Mo Thorium Analysis Results

Sample ID	Th-232		Th-230		Th-228	
	dpm/g-alloy	±1sigma	dpm/g-alloy	±1sigma	dpm/g-alloy	±1sigma
Bottom 1	0.95	±0.34	541.74	±8.02	803.17	±9.77
Bottom 2	0.48	±0.20	505.63	±6.37	751.24	±7.76
Bottom 3	0.25	±0.15	541.30	±6.76	802.68	±8.23
Top 1	0.75	±0.27	537.29	±7.16	780.87	±8.63
Top 2	<Limit	<Limit	520.42	±6.67	746.40	±7.99
Mean	0.61	±0.25	529.27	±7.02	776.87	±8.51

Table 10. Alpha Spectroscopy LEU U-10Mo Transuranic Analysis Results

Sample ID	Np-237		Pu-238		Pu-239+240	
	dpm/g-alloy	±1sigma	dpm/g-alloy	±1sigma	dpm/g-alloy	±1sigma
Bottom 1	367.14	±2.80	164.07	8.28	563.50	15.33
Bottom 2	366.22	±2.30	101.06	5.33	316.94	9.44
Bottom 3	398.59	±2.46	159.45	6.87	542.56	12.66
Top 1	394.46	±2.60	168.91	7.52	529.73	13.30
Top 2	398.09	±2.48	218.14	8.08	714.24	14.62
Mean	384.90	±2.53	162.33	±7.30	533.39	±13.23

Figure 12, Figure 13, and Figure 14 present the Bottom 1 sample thorium, neptunium, and plutonium alpha spectra, respectively. From the spectra, is clear the ingrowth of short half-life progeny (Ra-224, Rn-220, Po-215, and others) will depend on the presence and concentration of the nuclides identified in Table 3. The spectra for the rest of the samples analyzed are not included here because they are identical to the ones shown.

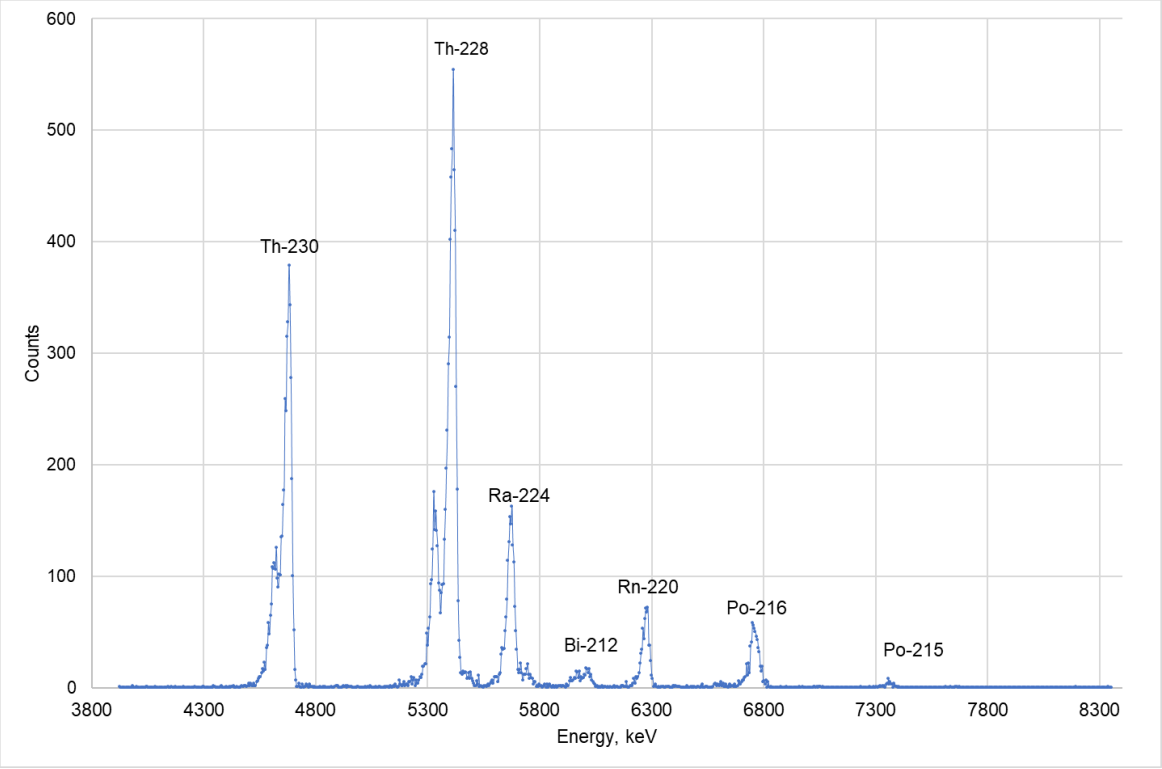

Figure 12. Bottom 1 Sample Thorium Analysis Results

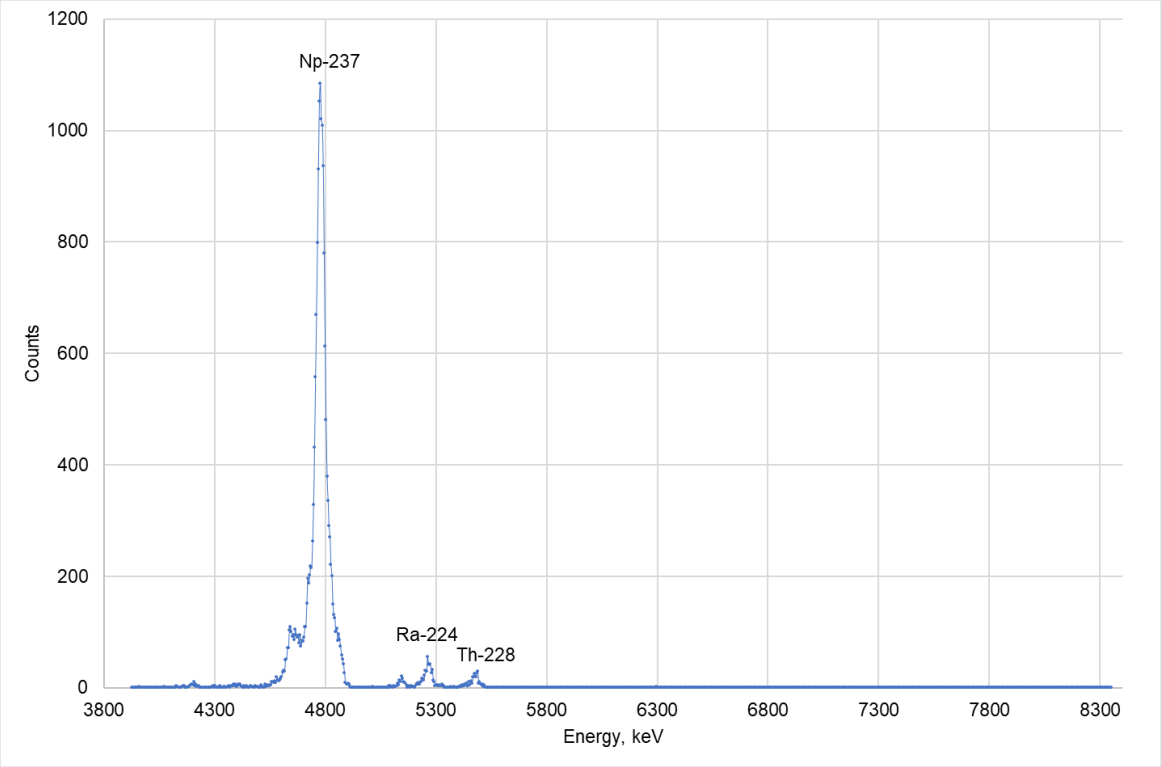

Figure 13. Bottom 1 Sample Neptunium Analysis Results

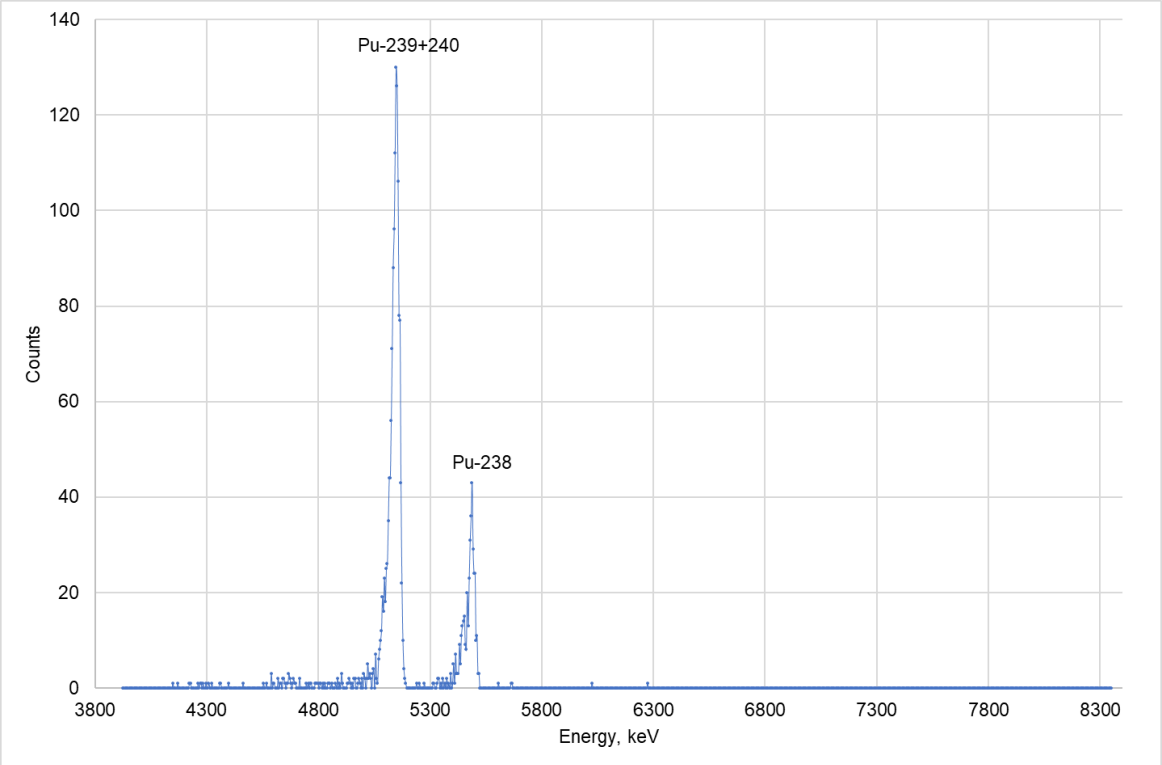

Figure 14. Bottom 1 Sample Plutonium Analysis Results

4.2 Contamination Levels and Progeny Diffusion After Thermal Treatment Results

4.2.1 Radiological Survey of Homogenized Sample

Table 11 presents the bottom-sample, post-homogenization radiological survey results. The beta-to-alpha activity ratio is 1.50, compared to 0.69 before homogenization. These results can be explained in terms of diffusion of the main beta-emitting decay products Th-234/Pa-234m and Th-231, and hence increases in their concentration toward the surface of the alloy.

Table 11. Post-Homogenization Bottom Sample Radiological Survey Results. Pre-homogenization mass of bottom sample (55.9 g) was reduced to 27.94 g (Table 4, Table 8, and Table 13).

	Unit	β-γ Background	α Background
Counts	counts	2628	31
Time	minutes	5	5
Count Rate	cpm	525.6	6.2
Standard Deviation	cpm	10.3	1.1
		β-γ Gross Counts at Contact	α Gross Counts at Contact
Counts	counts	346,912	114,991
Time	minutes	1	1
Count Rate	cpm	346,912	114,991
Standard Deviation	cpm	589.0	339.1
		β-γ Net Count Rate at Contact	α Net Count Rate at Contact
Count Rate	cpm	346,386	114,984.8
Standard Deviation	cpm	589.1	339.1
CV	%	0.17%	0.29%
r>1.65*sigma	cpm	972.0 (Yes)	559.5 (Yes)
		β-γ Activity at Contact	α Activity at Contact
Net Count Rate	cpm	346,386	114,984.8
Efficiency[a]	cpm/dpm	0.294	0.146
Efficiency (standard deviation)[b]	cpm/dpm	0.0001	0.0001
Activity	dpm	1,178,185	787,567
	Bq	19,636	13,126
Standard Deviation	dpm	2,004	2,323
	Bq	33	39
Beta-to-Alpha Activity Ratio		1.5:1	

[a] Efficiency based on calibration reports. The beta-gamma efficiency was taken based on Sr-90/Y-90 calibration source and the alpha efficiency was taken from Pu-239.
[b] This value was assumed to be small.

A *t*-test comparing the net count rates of the bottom sample before (Table 6) and after homogenization indicated more than 95% confidence that the beta/gamma and alpha net count rates are significantly higher after homogenization (i.e., post-heat treatment).

The alpha net count rates were about 12% higher in the bottom sample after homogenization, while the net beta/gamma count rates were about 2.5 times higher than the corresponding counts in the sample before homogenization. This can be attributed to diffusion of the beta and alpha decay products. It is important to note that the bottom sample that was homogenized had about 51% less mass than the sample radiologically surveyed (see Table 5) because samples were cut from it for the experiments described in Sections 4.1.4 and 4.2.2. These results mean that if the samples had the same mass, the increase in alpha and beta/gamma count rates would be higher.

These results indicate that the contamination levels at the surface of the LEU U-10Mo alloy increase with homogenization (i.e., thermal treatment).

The surface also was surveyed in the ionization chamber survey meter for beta dose rates. The results were identical to those presented in Table 7. This possibly indicates that beta particles contributing to the increase in the number of counts do not have enough energy to pass the 7 mg/cm^2 shield thickness of the ion chamber. This phenomenon will be analyzed more thoroughly in future research.

4.2.2 Progeny Analysis After Homogenization

After homogenization, the top sample came from the furnace with a canoe shape toward the edges (Figure 15). Table 12 presents the dimensional measurements performed for the samples before etching for depth-based analysis. For the top sample, the thickness was averaged between the edge and the midpoint. The top surface of the sample sagged in the middle. The sample thickness was 0.2010" at its edge and 0.1195" at its middle, resulting in an average thickness of 0.1603 inch (0.4070 cm).

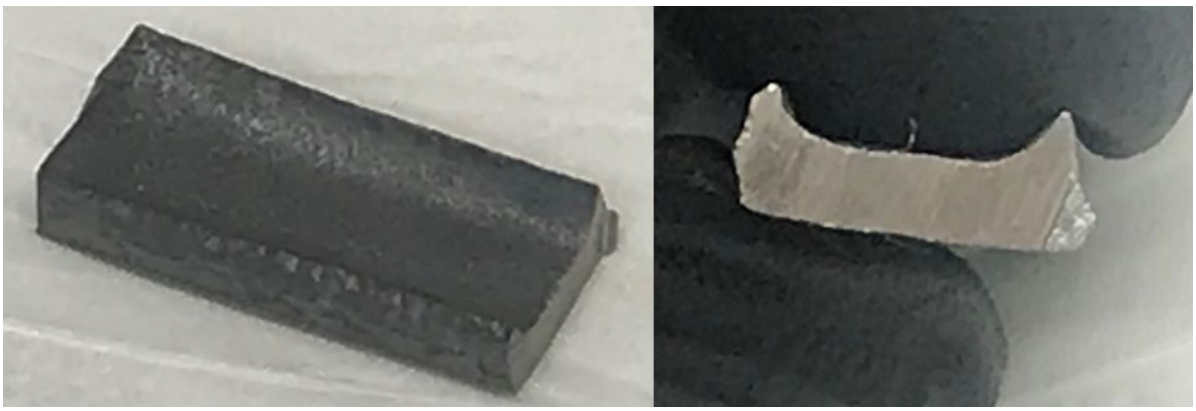

Figure 15. Top Sample after Homogenization. Left: longitudinal view; right: cross-sectional view

Table 12. Dimensional Measurements of Samples before Surface Etching[2]

Sample ID	Length (cm)	Width (cm)	Thickness (cm)	Volume (cm^3)
Homogenized Top	2.8105	1.2840	0.4070	1.4688
As-Cast Bottom	2.6251	1.2243	0.5156	1.6571

Table 13 shows the stepwise approach and etched-layer calculation. For each step, the difference in weight provides the mass etched and allows calculation of an approximate depth removed from each surface. The volume and depth calculations for the top sample are extremely rough, because the uneven shape of the sample after homogenization precludes simple calculations.

Table 13. Mass and Depth Estimation Measurement as a Function of Etching

Source	Layer Etched	Start Mass (g)	End Mass (g)	Mass Etched (g)	Approximate Volume Left (cm^3)	Approximate Depth (microns)
Piece of Homogenized Top Sample	Surface Layer	18.1216	18.0474	0.0742	1.4628	5.7000
	Subsurface Layer	18.0474	17.9740	0.0734	1.4569	5.6000
	Deeper Layer	17.9740	17.9035	0.0705	1.4512	5.5000
Piece of As-Cast Bottom Sample	Surface Layer	26.8198	26.7100	0.1098	1.6503	6.5500
	Subsurface Layer	26.7100	26.6030	0.1070	1.6437	6.4000
	Deeper Layer	26.6030	26.4977	0.1053	1.6372	6.3000

The objective of this part of the experiment was to etch the same layer depth off each piece each time. This was complicated by the uneven shape of the top piece after homogenization. The bottom sample was etched first, until approximately 0.1 g of U-10Mo was removed from the sample. The basis for this amount was ease of handling. Calculations showed that about 6.5 microns of material was removed from the surface. The top sample then was etched so the mass removed would be in the same proportion to the starting material as that of the bottom sample, using the assumption that this would remove approximately the same depth of material. For the next layers, a mass goal was calculated to maintain the same layer depth as the first etch. Because of the uneven and slightly unpredictable etch rates, the mass removed was typically within ±5 µm of the calculated goal.

The solution containing the top and deeper etched layers for each sample were surveyed with a 43-93 Ludlum alpha-beta probe. The detector was placed on the top of each vial and counted for 1 minute. The alpha counts were within background levels, presumably because of self-shielding within the liquid, air, and vial, but beta-gamma counts were detected, showing more activity in the solution etched from the surface of the top sample that had been homogenized. These results are presented in Table 14. In the top, homogenized sample, the net count rate doubled at the surface compared to the rate detected from the deeper layers, while in the bottom, as-cast sample, the activity remained almost identical among layers.

[2] The actual shape of the top cut piece was irregular, having a canoe shape toward the edges.

Table 14. Survey Results to Fraction Mass Etched in Dilution

Source	Layer Etched	Counts (per minute)	Net Count Rate (cpm)	Standard Deviation	CV %
Piece of Homogenized Top Sample	Surface Layer	1,550	426	51.71	12
	Subsurface Layer*	n/a	n/a	n/a	n/a
	Deeper Layer	1,344	220	49.68	23
Piece of As-Cast Bottom Sample	Surface Layer	1,508	384	51.30	13
	Subsurface Layer	n/a	n/a	n/a	n/a
	Deeper Layer	1,488	364	51.11	14
Background		1,124	1,124	33.53	3

*Subsurface layer values were not taken.

4.2.3 Gamma Spectroscopy Results

Table 15 and Table 16 present the results of duplicate gamma spectroscopy performed on each layer etched. The samples were corrected for the mass etched and the time since the Th-234/Pa-234m was separated from U-238 by anion exchange.

Results show higher Th-234/Pa-234m activity in the etched layers of the top sample after homogenization (i.e., heat treatment) than in layers of the as-cast bottom sample (not heat treated). This phenomenon is more prevalent at the surface and indicates that the increase in beta/gamma net count rates presented in Table 11 is from the U-238 beta decay products.

4.2.4 Alpha Spectroscopy Results

Table 17 presents the alpha spectroscopy results for the layers etched. The samples were corrected for mass and the time since the thorium nuclides were separated from their uranium parent by anion exchange (i.e., 47 days). In the case of Po-215 activity, no time correction was applied because the activity values in-grow from Ac-227 → Th-227 → Ra-223 → Rn-219. With some radon escaping, it is expected this activity is higher than reported.

These results demonstrate more uranium decay products or activity in the layers etched from the top, homogenized sample than layers from the bottom, as-cast sample. Progeny diffusion through the alloy is present.

Figure 16 shows the surface-etched alpha spectra for the top (homogenized) and bottom (as-cast) samples. Even though the top sample had less mass etched than the bottom sample (Table 13), the spectra show a considerable increase in counts from the surface layer of the top, homogenized sample compared to the bottom, as-cast sample.

Figure 17 and Figure 18 show the alpha spectra for the subsurface and deeper layers for the top, homogenized and bottom, as-cast samples. The spectra show lower counts from the homogenized sample than from the bottom, as-cast sample. This phenomenon can be attributed to a combination of lower mass etched through the deeper layers and a depletion-diffusion phenomenon in which the progeny elements diffuse to the upper layers. Note that the count scale of the plots in these figures is lower by a factor of 2–4 compared to the counts reported in Figure 16.

Table 15. Gamma Spectroscopy First-Measurement Results Analysis of Th-234/Pa-234m

Layer Etched	Sample ID	Mass (g)	Mass Correction Factor	Activity Measured (Bq)	Activity, Mass Corrected (Bq)	Activity, Decay Corrected (Bq)	Uncertainty (Bq)	CV (%)
Surface	Top Piece (Homogenized)	0.0742	1.4798	786.0	1,163.1	1,232.0	±27.4	2.2
	Bottom Piece (As Cast)	0.1098	1.0000	717.0	717.0	759.5	±18.8	2.5
Subsurface Layer	Top Piece (Homogenized)	0.0734	1.4578	551.0	803.2	850.8	±22.5	2.6
	Bottom Piece (As Cast)	0.1070	1.0000	730.0	730.0	773.2	±18.4	2.4
Deeper Layer	Top Piece (Homogenized)	0.0705	1.4936	545.0	814.0	862.2	±17.3	2.0
	Bottom Piece (As Cast)	0.1053	1.0000	681.0	681.0	721.3	±17.4	2.4

Table 16. Gamma Spectroscopy Second-Measurement Results Analysis of Th-234/Pa-234m

Layer Etched	Sample ID	Mass (g)	Mass Correction Factor	Activity Measured (Bq)	Activity, Mass Corrected (Bq)	Activity, Decay Corrected (Bq)	Uncertainty (Bq)	CV (%)
Surface Layer	Top Piece (Homogenized)	0.0742	1.4798	531.0	785.8	1,175.3	±20.4	1.7
	Bottom Piece (As Cast)	0.1098	1.0000	514.0	514.0	768.8	±13.1	1.7
Subsurface Layer	Top Piece (Homogenized)	0.0734	1.4578	402.0	586.0	876.6	±8.9	1.0
	Bottom Piece (As Cast)	0.1070	1.0000	518.0	518.0	774.8	±5.0	0.6
Deeper Layer	Top Piece (Homogenized)	0.0705	1.4936	395.0	590.0	882.5	±6.5	0.7
	Bottom Piece (As Cast)	0.1053	1.0000	476.0	476.0	712.0	±5.7	0.8

Table 17. Alpha Spectroscopy Results and Analysis

Isotope	Layer Etched	Sample ID	Mass (g)	Mass Correction Factor (g)	Activity Measured (dpm/sample)	Activity, Mass Corrected (dpm/sample)	Activity, Decay Corrected (dpm/sample)	Uncertainty of Activity Decay Corrected (dpm/sample)	CV (%)
Th-230 (From U-234)	Surface	Top Piece (Homogenized)	0.0742	1.4798	33.86	50.10	50.1	±1.02	2.0
		Bottom Piece (As Cast)	0.1098	1.0000	27.99	28.0	28.0	±0.86	3.1
	Subsurface Layer	Top Piece (Homogenized)	0.0734	1.4578	22.65	33.0	33.0	±1.12	3.4
		Bottom Piece (As Cast)	0.107	1.0000	30.44	30.4	30.4	±0.85	2.8
	Deeper Layer	Top Piece (Homogenized)	0.0705	1.4936	22.73	34.0	34.0	±1.15	3.4
		Bottom Piece (As Cast)	0.1053	1.0000	26.59	26.6	26.6	±0.79	3.0
Po-215 (From U-235)	Surface	Top Piece (Homogenized)	0.0742	1.4798	25.3	37.5	37.5	±0.87	2.3
		Bottom Piece (As Cast)	0.1098	1.0000	2.2	2.2	2.2	±0.24	11.0
	Subsurface Layer	Top Piece (Homogenized)	0.0734	1.4578	3.6	5.3	5.3	±0.45	8.5
		Bottom Piece (As Cast)	0.107	1.0000	1.6	1.6	1.6	±0.19	12.4
	Deeper Layer	Top Piece (Homogenized)	0.0705	1.4936	2.0	2.9	2.9	±0.34	11.5
		Bottom Piece (As Cast)	0.1053	1.0000	1.3	1.3	1.3	±0.17	13.5
Th-228 (From U-232/ U-236)	Surface	Top Piece (Homogenized)	0.0742	1.4798	54.00	79.9	83.9	±0.92	1.1
		Bottom Piece (As Cast)	0.1098	1.0000	41.96	42.0	44.1	±0.25	0.6
	Subsurface Layer	Top Piece (Homogenized)	0.0734	1.4578	34.86	50.8	53.4	±0.47	0.9
		Bottom Piece (As Cast)	0.107	1.0000	42.75	42.7	44.9	±0.20	0.5
	Deeper Layer	Top Piece (Homogenized)	0.0705	1.4936	34.56	51.6	54.2	±0.35	0.7
		Bottom Piece (As Cast)	0.1053	1.0000	39.50	39.5	41.5	±0.18	0.4

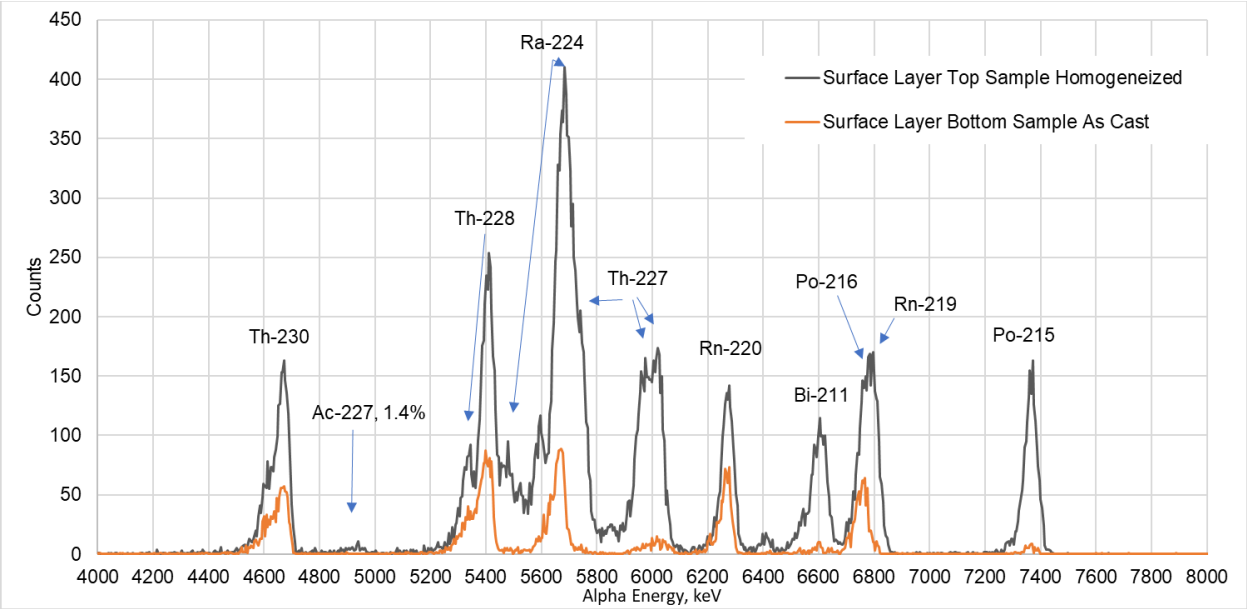

Figure 16. Thorium Alpha Spectrum for Surface Layer Etched from Homogenized Top Sample and As-Cast Bottom Sample

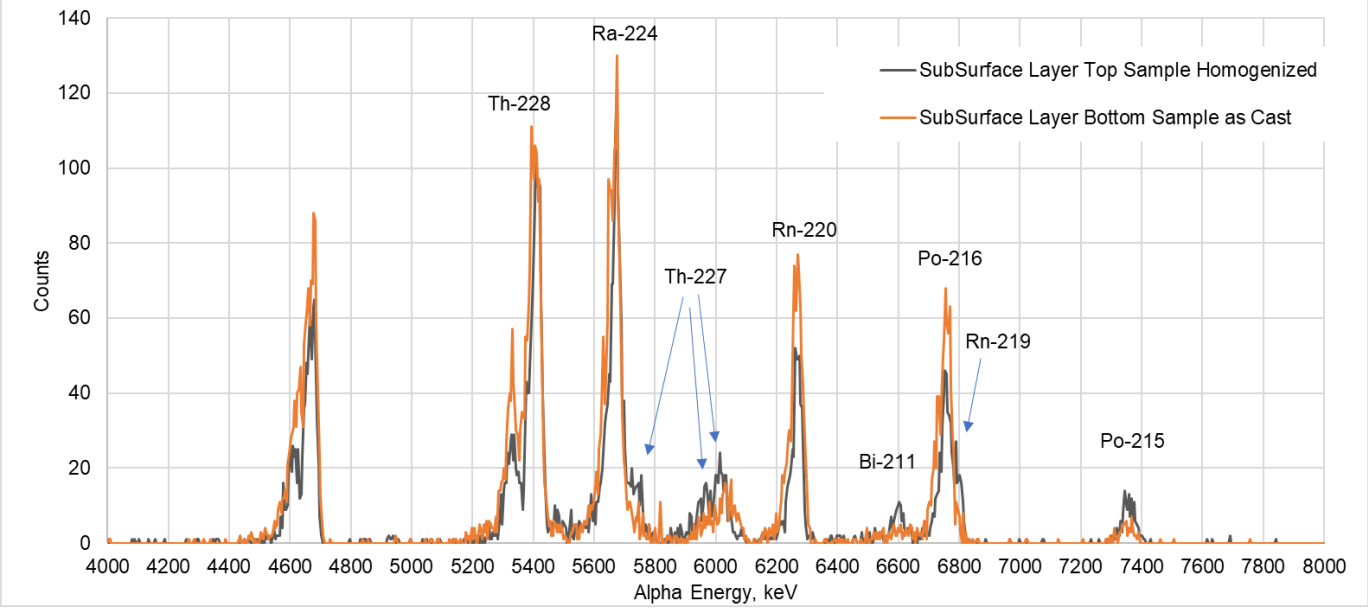

Figure 17. Thorium Alpha Spectrum for Subsurface Layer Etched from Homogenized Top Sample and As-Cast Bottom Sample

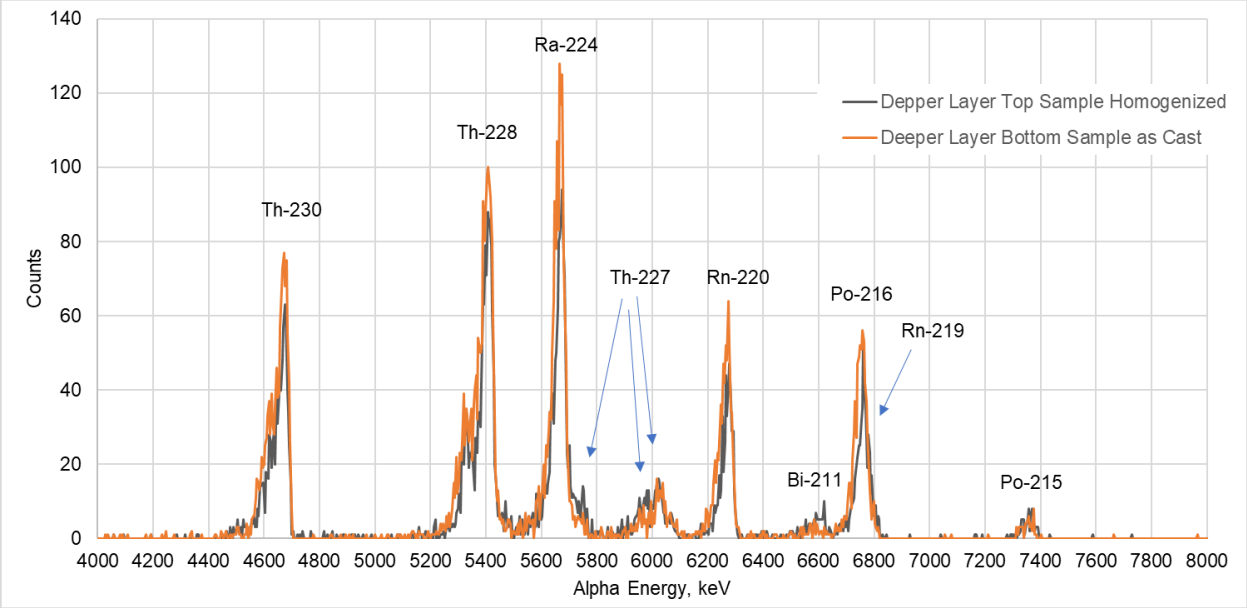

Figure 18. Thorium Alpha Spectrum for Deeper Layer Etched from Homogenized Top Sample and As-Cast Bottom Sample

4.2.5 Continuous Air Monitoring Results

Table 18 presents the CAM event definitions. The experiment period extended from late April to June of 2021.

Figure 19 presents the integrated counts per minute with the events identified in Table 18. The fluctuations observed in chart as primary attributed to air changes in the glovebox when samples were inserted, and normal background fluctuations in the building. Note the counts scale is low.

Table 18. CAM Event Definitions

Event	Timing		Delta (minutes)
Background	Start Date	4/23/21 3:00 PM	5,370
	Finish Date	4/27/21 8:30 AM	
Top Sample As-Cast	Start Date	4/27/21 8:45 AM	33,420
	Finish Date	5/20/21 1:45 PM	
Background	Start Date	5/27/21 3:30 PM	11,085
	Finish Date	6/4/21 8:15 AM	
Top Sample After Homogenization	Start Date	6/4/21 8:30 AM	26,085
	Finish Date	6/22/21 11:15 AM	

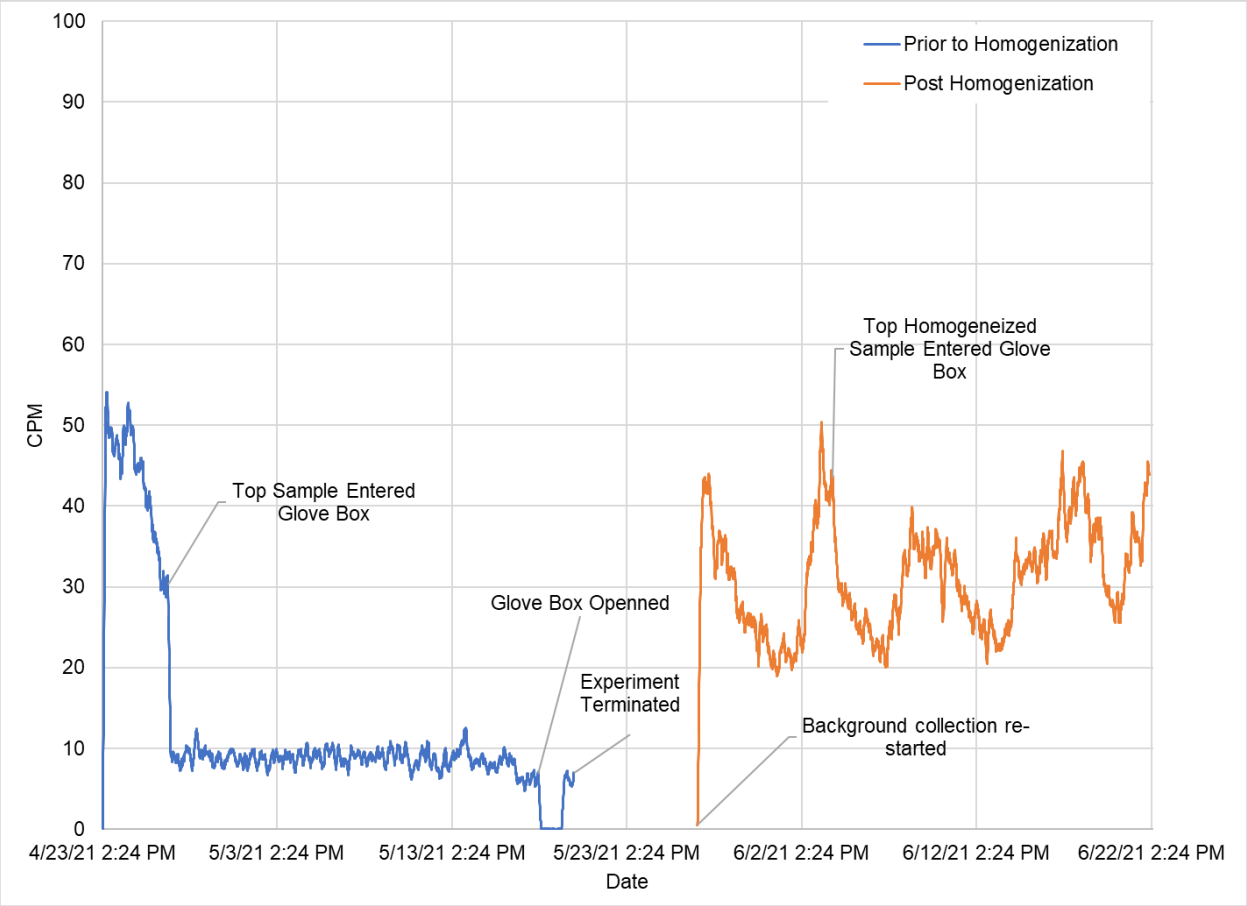

Figure 19. CAM as a Function of Time/Progression of Events. CPM is counts per minute.

5.0 Conclusions

This research focused on the radiological characteristics and diffusion of uranium decay products as a function of homogenization in LEU U-10Mo alloy. In the homogenization step, the alloy was thermally heat treated in a VAF at 1 mTorr for 140 hours at 900°C.

From the results presented in Section 4.0, the following conclusions were drawn:

- Before heat treatment (homogenization), the top sample had higher surface beta/gamma and alpha count rates than the plate's bottom sample. The Army Materiel Command handbook for DU (AMC 1989) associated this phenomenon with the top section of the plate, (usually called “the hot top”), where the concentration of the uranium decay products is higher than in the bulk. However, the top sample analyzed in this work did not come from the hot top section of the plate; instead, it came from the upper section of the plate. This result points to a possible gradient of uranium decay products, where the concentration of decay products is higher at the top of a plate and decreases toward the bottom. It is important to note that this cast plate resulted from a short pour, which means the hot top was not generated. Future research will be proposed to better study this phenomenon during plate formation for the LEU U-10Mo fuel.
- The beta/gamma dose rate was 66 mrad/h at contact with the surface of the alloy. The beta particles most likely came from Th-234/Pa-234m (2.29 MeV end-point energy). The beta dose rate is lower than that of DU (AMC 1989) and in the range shown in DOE (2000) for uranium enriched to 19.75 wt% U-235. This lower value was expected. The beta dose rate should decrease with increasing enrichment because of a lower beta particle contribution from Th-234/Pa234m (from U-238); the fuel is 90 wt% uranium and self-shielding occurs due to the presence of molybdenum (10 wt%).
- The LEU U-10Mo gamma and alpha spectroscopy analysis indicates the following:
  - Recycled uranium is present. The main external radiological concern is U-232 decay products. These products can reach equilibrium relatively quickly (~10 years) compared to U-238 or U-235 decay products. Of particular importance is the ingrowth of Tl-208, which produces gamma rays of 2.614 MeV and 0.584 MeV, with 100% and 96 per disintegration, respectively.
  - No significant variation in the activity analysis of the alpha emitters between the top and bottom samples was found for the evaluated Th-230 and Th-228 progeny and transuranic elements. For the as-cast (i.e., unhomogenized) condition, lighter progeny can be segregated by gravity, but this occurs only on the surface of the casting, not inside it.
- Initial data indicate that the progeny may increase from when the fuel is cast (i.e., a minimum contribution from feedstock aging). The lowest radioactivity is predicted in the fresh samples of LEU U-10Mo alloy, and it will increase over time because uranium will continue to decay and generate progeny (i.e., Th-231, Th-234/Pa-234m, Th-230, Th-228, and others).
  - The alpha spectroscopy results clearly showed ingrowth of Th-228, Ra-224, Rn-220, Po-216 (daughters of U-232/236), and Th-230 (from U-234). The Th-230 activity ingrowth is approximately equal to the ingrowth expected from U-234 decay over two years. Polonium-215 in the alpha spectrum proves that Ac-227 and likely its parent, Pa-231, were also present.

After the sample was homogenized, the following were observed:

- The surface beta/gamma and alpha activity increased from the activity measured for the same sample before homogenization. Of significance, although the homogenized sample had 51% less mass, it exhibited more surface activity. The alpha activity increased by 12% and the beta/gamma activity increased by a factor of 2.5. The beta-to-alpha activity ratio also increased by a factor of 1.50.
  - Gamma spectroscopy results suggest the primary contributors are the U-238 decay products Th-234/Pa234m in the surface layer. The other etched layers show a “depletion profile” of these decay products and more activity overall than the sample that was not homogenized. Previous reports on DU castings pointed to the possibility of the surface having a prominent presence of the uranium decay products. (DOE 2000).
  - The homogenized top sample had more activity per etched layer than the bottom sample that was not homogenized. The activity is higher at the first surface etched from the top homogenized sample, while subsequent etched layers from the same sample seem to be “depleted” in decay products. The potential mechanism involved may be vacancy movements in the atoms. In these vacancy movements, atoms exchange positions or move cooperatively via grain boundary diffusion, chemical diffusion, and intrinsic diffusion coefficients. To reduce this diffusion phenomenon, future research will investigate which mechanism is most dominant.
- CAM results showed no difference from background when the top sample was monitored for a month before homogenization and a month after homogenization. It seems the quantity of the material, combined with the large volume of air (i.e., in the glovebox) contributed to not detecting a signal above the background level. Future research will redesign this experiment to better characterize the airborne contributions.

As the process scales up, it is crucial to understand how fabrication processes and variables will change the radiological characteristics of the alloy so radiological controls needed to meet regulatory requirements can be designed.

6.0 Quality Assurance

This work was performed in accordance with the Pacific Northwest National Laboratory Nuclear Quality Assurance Program (NQAP). The NQAP complies with United States Department of Energy Order 414.1D, *Quality Assurance*. The NQAP uses NQA-1-2012, *Quality Assurance Requirements for Nuclear Facility Application,* as its consensus standard and NQA-1-2012 Subpart 4.2.1 as the basis for its graded approach to quality.

This work emphasized acquiring new theoretical or experimental knowledge. The information associated with this report should not be used as design input or operating parameters without additional qualification.

7.0 References

Army Materiel Command (AMC). 1989. *Handbook of Safety Procedures for Processing Depleted Uranium*. AMC HDBK-385-1.1-89, Department of the Army, Washington, D.C.

Cember H, T Johnson. 2008. *Introduction to Health Physics*, Fourth Edition, The McGraw-Hill Companies, Inc. Pages 490-495. Accessed November 29, 2021, at https://inayacollegedrmohammedemam.files.wordpress.com/2015/02/introduction-to-health-physics.pdf.

COC WR 866218 – Consolidated Nuclear Security LLC. 2019. *Certificate of Conformance U-Mo Ingot Manufacturing and Quality Plan for Plate Demonstrations*, Work Request 866218, Y-12 National Security Complex, Oak Ridge, Tennessee.

Darken, LS and RA Oriani. 1954. "Thermal Diffusion in Solid Alloys." *Acta Metallurgica* 2:6, 841-847. Accessed November 29, 2021, at https://doi.org/10.1016/0001-6160(54)90038-3.

DOE – U.S. Department of Energy. 1994. *Airborne Release Fractions/Rates and Respirable Fractions For Nonreactor Nuclear Facilities*. DOE Handbook DOE-HDBK-3010-94, Washington, D.C. Accessed November 29, 2021, at https://www.standards.doe.gov/standards-documents/3000/3010-bhdbk-1994.

DOE – U.S. Department of Energy. 2017. *Guide of Good Practices for Occupational Radiation Protection in Uranium Facilities*. DOE-STD-1136-2017. U.S. Department of Energy, Washington D.C. Accessed November 29, 2021, at https://www.standards.doe.gov/standards-documents/1100/1136-AStd-2017

Hinnefeld SL, CR Lagerquist, WG Mansfield, LH Munson, and E R Wagner. 1988. *Health Physics Manual of Good Practices for Uranium Facilities*: Appendix A. EGG-2530, EG&G Idaho, Idaho National Engineering Laboratory, Idaho Falls, Idaho.

Idaho National Laboratory (INL). 2018. *Specification for Low Enriched Uranium Monolithic Fuel Plates*. SPC-1635, Rev. 10. Idaho National Laboratory, Idaho Falls, Idaho.

Idaho National Laboratory. 2019. *Supporting Information for the Low Enriched Uranium Monolithic Fuel Design*. SPC-1635, Rev. 6. Idaho Falls, Idaho.

Johnson T and B Birky. 2012. *Health Physics and Radiological Health Handbook*, Fourth Edition. Lippincott Williams & Wilkins, Baltimore, Maryland. Chapter 8, pages 459-465. Accessed November 29, 2021, at https://doi.org/10.1118/1.4826186.

Martin A, S Harbison, K Beach, and P Cole. 2012. *An Introduction to Radiation Protection*, Sixth Edition, Hodder Arnold, an imprint of Hodder Education, a division of Hachette UK, London. Pages 606-609.

Mehl RF. 1937. "Rates of Diffusion in Solid Alloys." *Journal of Applied Physics* 8:174. Accessed November 29, 2021, at https://doi.org/10.1063/1.1710280.

NRC – U.S. Nuclear Regulatory Commission. 2012. *Health Physics Surveys During Enriched Uranium-235 Processing and Fuel Fabrication*. Regulatory Guide 8.24, Revision 2. Washington, D.C.

Thomas J, J Mauro, J Rynicker, and R Fellman. 1979. *Airborne Uranium and Its Concentration and Toxicity in Uranium Enrichment Facilities*. k/PO/SUB-79/31057/1, Envirosphere Company, New York, New York, February 1979. Accessed November 23, 2021, at https://www.osti.gov/servlets/purl/12087141/.

Tsoulfanidis N. 1995. *Measurement and Detection of Radiation*. Second Edition, Taylor and Francis. Pages 64-68.

L'Annunziata, M, Vajda N., Martin P., Kim C. 2012. Handbook of Radioactivity Analysis, Chapter 6 Alpha Spectrometry. Third Edition, Elsevier Inc, pages 394-409.

Pacific Northwest National Laboratory

902 Battelle Boulevard
P.O. Box 999
Richland, WA 99354
1-888-375-PNNL (7665)

www.pnnl.gov